# *Large amplitude oscillatory shear flow of gluten dough: A model power-law gel*



**Citation:** Ng, Trevor S. K., Gareth H. McKinley, and Randy H. Ewoldt. "Large Amplitude Oscillatory Shear Flow of Gluten Dough: A Model Power-Law Gel." J. Rheol. 55, no. 3 (2011): 627.

**As Published:** http://dx.doi.org/10.1122/1.3570340

**Publisher:** American Institute of Physics

**Persistent URL:** http://hdl.handle.net/1721.1/87626

**Version:** Author's final manuscript: final author's manuscript post peer review, without publisher's formatting or copy editing

# Large Amplitude Oscillatory Shear Flow of Gluten Dough; A Model Power-law Gel

Trevor S. K. Ng[a], Gareth H. McKinley[a], and Randy H. Ewoldt[b]

*a) Hatsopoulos Microfluids Laboratory, Department of Mechanical Engineering, Massachusetts Institute of Technology, Cambridge, MA 02139, USA*

*b) Institute for Mathematics and its Applications & Department of Chemical Engineering and Materials Science, University of Minnesota, Minneapolis, MN 55455, USA*

January 18, 2011

## SYNOPSIS

In a previous paper [Ng and McKinley (2008)], we demonstrated that gluten gels can best be understood as a polymeric network with a power-law frequency response that reflects the fractal structure of the gluten network. Large deformation tests in both transient shear and extension show that in the absence of rigid starch fillers these networks are also time-strain factorizable up to very large strain amplitudes ($\gamma^* > 5$). In the present work, we further explore the non-linear rheological behavior of these critical gels by considering the material response obtained in large amplitude oscillatory shear (LAOS) over a wide range of strains and frequencies. We use a Lissajous representation to compare the measured material response with the predictions of a network theory that is consistent with the proposed molecular structure of gluten gels. In the linear viscoelastic regime, the Lissajous figures are elliptical as expected and can be quantitatively described by the same power-law relaxation parameters determined independently

from earlier experiments. In the non-linear regime, the Lissajous curves show two prominent additional features. Firstly a gradual softening of the network indicated by the rotation of the major axis. This feature is accounted for in the model by the inclusion of a simple non-linear network destruction term that reflects the reduction in network connectivity as the polymer chains are increasingly stretched. Secondly, a distinct upturn in the viscoelastic stress is discernable at large strains. We show that this phenomenon can be modeled by considering the effects of finitely extensible segments in the elastic network. We apply this model to other large amplitude transient flows such as the start-up of steady shear and extension. In addition to quantitative prediction of the evolution of stress in the gluten gel, we find that the onset of strongly non-linear unsteady phenomena such as edge instability in shear and sample rupture during extension can be understood as consequences of the finite extensibility and increased dissociation of the network filaments.

# I INTRODUCTION

The rheological responses of biopolymer networks exhibit an intriguing variety of nonlinear phenomena. Commonly observed features include nonlinear softening, stiffening, reversibility and thixotropy, e.g. [Chaudhuri *et al.* (2007); Ewoldt *et al.* (2007); Ma *et al.* (1999); Storm *et al.* (2005)]. There are a wide variety of measurement techniques and a range of constitutive models that have been proposed for understanding these types of systems [Chaudhuri *et al.* (2007); Gittes and MacKintosh (1998); Janmey (1991); Storm *et al.* (2005)]. In this article, we will illustrate some of these features observed in a viscoelastic biopolymer gel that is formed by a hydrated gluten network.

Gluten is the generic name given to the insoluble protein fraction present in wheat flour. It is widely believed that the mechanical properties of this hydrated network state are intrinsically linked to the quality of the bread dough formed when the flour is mixed with water [Belton (1999); Bloksma (1990b); Ewart (1989); Kokelaar *et al.* (1996); Schofield and Blair (1937); Singh and MacRitchie (2001); Uthayakumaran *et al.* (2000)]. Recent tests [Ng and McKinley (2008)] have shown that under small amplitude oscillatory conditions, as well as in large deformations in either shear or extension, the gluten gel can best be understood as consisting of flexible/semi-flexible segments that are interconnected to form a gel network. The interstitial spaces are filled with water but have minimal direct effect on the rheology as little or no solvent contribution to the total stress can be detected. For time scales that are greater than the Rouse relaxation time of the polymeric network segments, we also demonstrated that the quasi-linear behavior in an unfilled gluten gel is time-strain separable up to large strains and can be well-described by the generalized gel equation:

$$\sigma(t) = -\int_0^t S(t-t')^{-n} \frac{\partial}{\partial t'} \mathbf{C}^{-1}(t,t') dt' \tag{1}$$

where $\mathbf{C}^{-1}$ is the finger strain tensor. The expression can also be rewritten in terms of the finite strain rate tensor in the following way:

$$\sigma(t) = \int_0^t S(t-t')^{-n} \gamma_{[1]} dt' \tag{2}$$

where $\gamma_{[1]} = -\frac{\partial}{\partial t'} \mathbf{C}^{-1}$ [Bird *et al.* (1987a)].

Our previous studies also showed that in start-up of steady shear tests, both the transient shear stress and first normal stress difference exhibited power-law growth up to a critical strain $\gamma^* \sim 5$ at which point non-linear stress growth becomes significant and is followed rapidly by a viscometric instability leading to sample roll-up and ejection from the rheometer. The quasi-linear behavior before the instability is given by equation (1) which can be integrated for homogeneous steady shearing to give [Winter and Mours (1997); Ng and McKinley (2008)]:

$$\sigma_{xy}^{+}(\dot{\gamma}_0, \gamma) = \frac{S}{1-n} \dot{\gamma}_0{}^{n} \gamma^{1-n} \tag{3}$$

The transient extensional stress difference in strips of gluten undergoing uniaxial elongation also closely followed the predicted behavior up to the point of rupture; with the normal stress difference given by:

$$\Delta\sigma(\varepsilon) = S\dot{\varepsilon}_0^n \int_0^{\varepsilon} r^{-n} \left\{2\exp(2r) + \exp(-r)\right\} dr \tag{4}$$

derived from Eq. (1) with the change of variable $r = \dot{\varepsilon}_0 (t-t')$ . In general, the material functions for these start-up tests are of a time-strain factorizable form, in which the stress

response is separated into a rate-dependent component of power-law form multiplied by a master strain function:

$$\sigma(t) = S\dot{\gamma}^{n}\Phi(\gamma) \tag{5}$$

This separable form is appropriate for a range of deformation, but will ultimately fail when the network is deformed severely. Because of the difficulty in maintaining viscometric flow at large strains, the details of this progression into non-linear (non factorizable) behavior are still not well understood. There are clear hints of strain-hardening in the network, however during transient experiments in which the stress is always growing this large additional stress growth leads to sample disruption (either by ejection from the gap in shear or cohesive rupture in extension).

Unlike deformations in the linear viscoelastic regime, there exists no standard non-linear rheological test that can readily provide all the complex viscoelastic parameters which characterize the non-linear rheological behavior of a material such as these polymeric gels. Typically, different tests are employed to probe different aspects of the non-linearity. We suggest that large amplitude oscillatory shear (LAOS) deformation [Dealy and Wissbrun (1990)] is a useful tool for understanding polymeric gels. Large amplitude oscillatory deformations provide a number of rheometric advantages. Firstly, because the amplitude of oscillation can be progressively increased, we can probe deformation conditions close to the point of viscometric instabilities (e.g. immediately prior to the ejection of very elastic samples such as dough from the gap at large torsional strains). The measurements are taken under quasi-steady state; the imposed oscillations can be continued until any initial transient response has decayed and the shape of the resulting Lissajous, or more correctly 'Lissajous-Bowditch' curves [Bowditch (1815); Crowell (1981); Lissajous (1857)] remain time invariant, therefore the accuracy and repeatability are greatly improved when compared with transient start-up tests. Furthermore, the smoothly

varying deformation protocol can be precisely achieved experimentally, in contrast to the abrupt changes required for stress relaxation and start-up of steady flow tests. Also, since the tests are performed on conventional torsional rheometers, the experimental protocols are simpler and more convenient compared to non-linear tests involving large extensional deformations and/or high extensional rates such as filament stretching or wind-up tests [Ng *et al.* (2006); Rasmussen *et al.* (2008)]. Until recently, however, quantitative interpretation of the material response measured in a large amplitude oscillatory test has been far from obvious.

The experimental and analytical techniques of LAOS and Fourier transforms have been neatly summarized by Wilhelm (2002). Due to the conceptual familiarity of Fourier transforms, this framework of collecting and analyzing data is the most widely adopted. An alternative to Fourier analysis, based in the domain of strain and strain-rate rather than time, has been proposed by Cho *et al.* (2005). The method is based on symmetry arguments that decompose the Lissajous curves formed by parametric plots of stress as a function of strain and strain-rate into non-linear elastic and viscous components. More recently, Ewoldt and co-workers [Ewoldt *et al.* (2008)] have proposed a number of general measures of material moduli that capture the physical features embodied in Lissajous figures, and used these to generate a complete rheological fingerprint for a range of nonlinear viscoelastic materials such as wormlike micellar solutions and pedal mucus collected from snails and slugs.

To the best of our knowledge, the only published study in which gluten gels were subjected to large amplitude oscillations was performed by Uthayakumaran *et al.* (2002). Their experiments consisted essentially of a strain sweep at fixed frequency in which the strain amplitude was gradually increased and the corresponding dynamic moduli were reported ($G'(\omega;\gamma_0), G''(\omega;\gamma_0)$, which were presumably the first-harmonic moduli typically output from

commercial rheometer software). The data show a gradual decrease in moduli for increasing strains that was interpreted as a strain-softening behavior. Although this captures one global feature of the nonlinear network deformation, as we shall discuss later, reporting the apparent strain-dependent moduli of a soft nonlinear solid is not sufficient to fully characterize the rheological response of the network. A single harmonic measure such as the first harmonic moduli $G_1'$, $G_1''$, cannot adequately capture the complete response of the system [Ewoldt *et al.* (2008); Wilhelm (2002)] if it is not discussed in context with the Lissajous curves or a more detailed Fourier decomposition of the stress-strain response during an oscillation cycle.

Lefebvre (2006) studied the Lissajous figures resulting from LAOS deformation of wheat flour dough which is a more complex system than a gluten gel due to the presence of the starch filler. The experiments were performed on a controlled stress rheometer, in which the oscillatory stress amplitude was gradually increased. Lefebvre analyzed the corresponding strain response in terms of a Fourier series and he suggested that the relative magnitude of the higher harmonics could be considered to be a measure of the non-linearity. Although this Fourier decomposition approach is complete and mathematically consistent [Wilhelm (2002)], it is difficult to develop a clear physical interpretation of these higher harmonic components. Furthermore, the controlled stress nature of these experiments makes it inconvenient to compare data against candidate constitutive equations in which the material stress is commonly written as a non-linear function of input strain or strain rate. Nevertheless, the Lissajous figures presented by Lefebvre do indeed show distinct non-linear behavior, the most prominent being the dramatic distortion from the elliptical shapes observed at moderate stresses (i.e. $\sigma_0 \geq 100$ Pa ) and small strains ( $\gamma_0 \sim 0.05$ ).

Phan-Thien *et al.* (2000) on the other hand performed large amplitude oscillations on a wheat flour dough using a controlled strain approach. As a result, they were able to propose a

constitutive equation that described the extreme softening behavior observed when the dough is subject to increasingly large strains ($\gamma_0 > 1\%$). The resulting constitutive model [Phan-Thien *et al.* (2000); Phan-Thien *et al.* (1997)] consists of a factorizable form with a linear viscoelastic response multiplied by an empirical softening function that is dependent on the strain. Flour dough is a highly-filled suspension with a viscoelastic matrix and the onset of nonlinearity occurs at very small strains (0.1%) as compared to isolated (unfilled) gluten dough (3%) [Uthayakumaran *et al.* (2002)]. Thus, for flour dough, it is currently unclear how much of the nonlinearity can be attributed directly to the polymeric gluten gel network.

In the present work we study the non-linear rheological behavior of a model biopolymer network consisting of hydrated gluten using controlled-strain large amplitude oscillatory shear flow. Following the earlier work of Lefebvre (2006) and Phan-Thien *et al.* (2000), we analyze the Lissajous figures of the gluten gel resulting from controlled oscillatory forcing under various deformation amplitudes and frequencies. The experimental data collected are used to extend the generalized gel constitutive model described above to describe the progressive transition to non-linear behavior that is observed experimentally. This model is based on the transient network ideas described in our earlier work [Ng and McKinley (2008)] and we then explain how each of the characteristic rheological features observed in the LAOS experiments arise from underlying changes in the microstructure of the gluten gel network.

# II GLUTEN DOUGH PREPARATION

Gluten dough was prepared by placing 10g of vital gluten (Arrowhead Mills, ~12% moisture content) in a mixograph bowl with 14g of water (total dough moisture content = 63% by weight). The mixture is then stirred, stretched and folded through the action of the mixograph pins for 12 minutes [Gras *et al.* (2000)]. The torque exerted by the mixing action is monitored on a specially instrumented mixograph. In Figure 1 (a), we plot the typical torque signal as a function of mixing time. Frequently, a moving average signal corresponding to the slow variation of torque is cited to be indicative of dough development [Bloksma (1990b)]. The various stages of development can be summarized by the following:

i. 0 – 500 s. Under-developed dough – mixing torque is low. The sample is dry and lumpy.

ii. 500-600 s. Dough development – both the local average torque signal and amplitude of fluctuations rise rapidly. Sample begins to form a cohesive dough that is stretched around the mixograph pins.

iii. 600-900 s. Fully-developed dough – the amplitude of the averaged torque signal and the corresponding fluctuations reach a plateau. Gluten samples harvested at this stage give consistent results under rheometric tests. An enlarged detail of the fluctuations of the signal at this stage of development is shown in Figure 1 (b).

iv. > 900 s. Over-developed dough – gradual decrease of torque signal. Dough samples collected at this stage are believed to have weak "functionality" [Bloksma (1990b)].

In fact, the mixing motion can be thought of as a composite series of large amplitude oscillatory tests. The epitrochoidal motion of the mixograph pins are given in Cartesian coordinates with origin at the center of the mixing bowl by the following equations [Buchholz (1990)]:

$$x = r_1 \cos(\theta + \theta_i) + r_2 \cos\left\{\left(1 + \frac{n}{m}\right)\theta + \phi_i\right\}$$
$$y = r_1 \sin(\theta + \theta_i) + r_2 \sin\left\{\left(1 + \frac{n}{m}\right)\theta + \phi_i\right\} \quad (6)$$

where $r_1$ = 1.78cm, $r_2$ = 0.89cm, and $n/m$=3/4 are the geometric parameters of the mixograph with four moving pins positioned at $(\theta_i, \phi_i)$ = (0,0), (0,π), (π, 1/4π), (π, 5/4π) respectively. The resulting deformation imposed on the dough by the four moving pins whirling around the three stationary pins is extremely complicated, and we show the contributions to the power spectrum of this epitrochoidal pin motion in Figure 1 (c) by the broken lines. This power spectrum is calculated from the kinematic function that describes the distances between each of the moving pins with respect to the stationary pins. The transfer function that transforms the kinematic input of the rotating pins into the measured torque output is provided by the gluten gel itself, and results in the torque spectrum shown by the solid line in Figure 1 (c). It is this rheological response that we ultimately seek to characterize. A number of the kinematic peaks are clearly identifiable in the corresponding power spectrum computed from the measured torque response. The harmonic content of the mixograph deformation history is too complex to analyze systematically. However, the periodic nature of the deformation suggests that we naturally should seek to decompose the system response into contributions that depend on the strain amplitude and deformation frequency using the concept of large amplitude oscillatory shear flow (LAOS).

## III RHEOMETRY

Shear rheometry experiments were performed under controlled strain conditions on the ARES rheometer and also under controlled stress conditions on the AR-G2 rheometer (TA instruments). A Peltier plate and a 25mm parallel plate fixture with 1mm gap separation were used in all tests. Approximately 2 g of the freshly-mixed gluten dough was placed on the Peltier plate, and the upper plate was then brought down to compress the sample to the specified thickness. Excess dough was trimmed with a razor blade. The Peltier plate was held at a fixed temperature of 22ºC, to represent typical room temperature. Slip was eliminated by applying adhesive-backed sandpaper (600 grit McMaster Carr 47185A51) to the surfaces of both the Peltier plate and the parallel plate tool. Drying of the sample at the outer edges was minimized by painting the exposed surface of the dough with a low-viscosity silicone oil. Additional details and the results of both linear viscoelastic characterization and startup tests in shear and extension are reported elsewhere [Ng and McKinley (2008)].

## IV LINEAR VISCOELASTICITY AND NETWORK STRUCTURE OF GLUTEN GELS

We begin by outlining the key features of gluten gel viscoelasticity elucidated in our previous publication [Ng and McKinley (2008)]. In that study we showed that the gluten gel forms a polydisperse network of macromolecular strands held between junction points. This polydispersity is reflected in the power-law like relaxation function which can be visualized as a series of Maxwell modes capturing the response of the fractal gel at different length and time scales. The fundamental material response can be decomposed into two regimes. At low

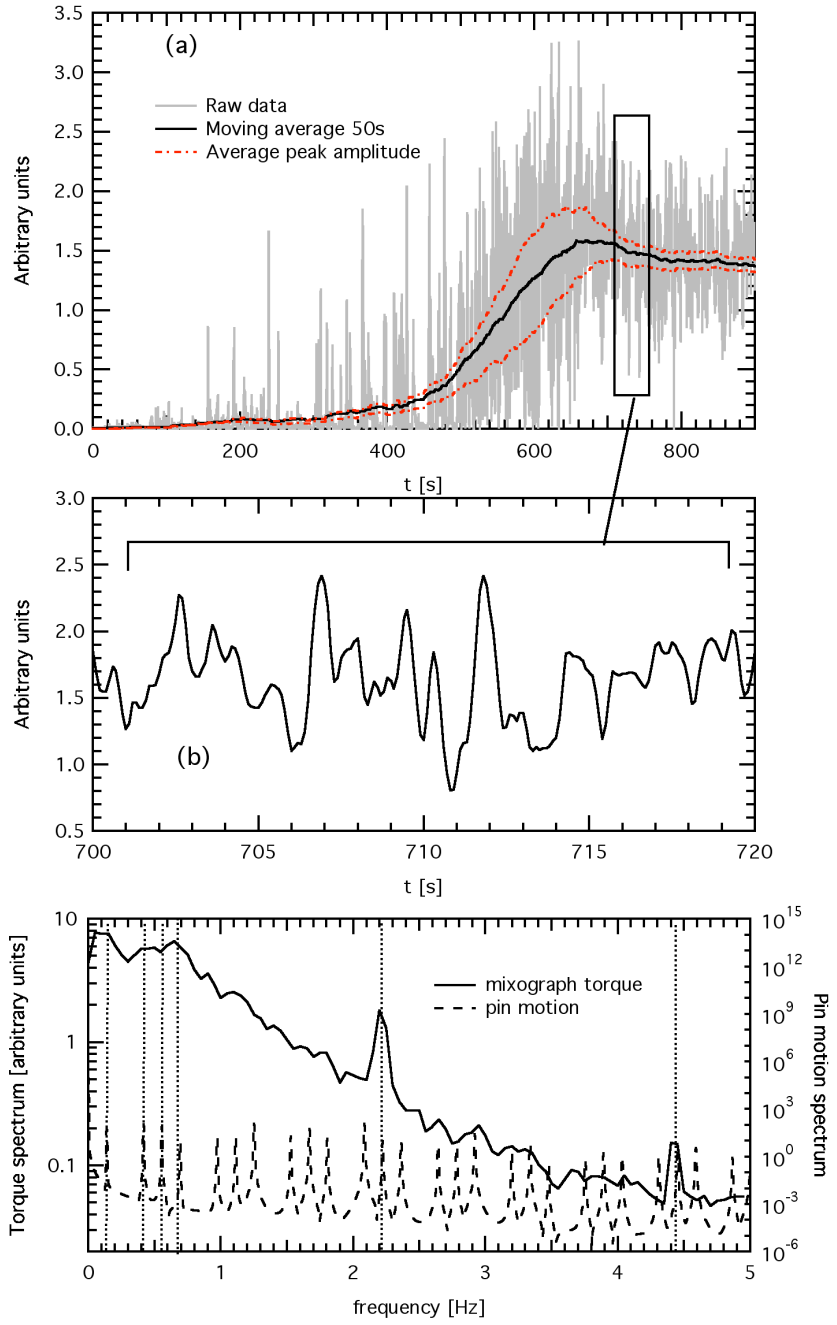


Figure 1 (a) Measured mixograph output (torque in arbitrary units) vs. mixing time for a typical gluten dough. (b) Detail of temporal oscillations in the measured torque signal from 700-720s due to the periodic motion of the pins. (c) Power spectrum of the measured mixograph torque (solid line) from 700-800s. Peaks correspond to harmonics calculated from the epitrochoidal motion of the four moving pins in relation to the three stationary pins in the mixograph bowl.

frequencies ($\omega < 20$ rad s$^{-1}$), the linear viscoelastic properties of the gluten dough exhibit a critical-gel–like behavior, as shown in Figure 2 [Chambon and Winter (1987); Winter and Chambon (1986); Winter and Mours (1997)], in which the dynamic moduli are power-law functions of the imposed frequency and are inter-related by the following simple expression:

$$G'_{gel}(\omega) = \frac{G''_{gel}(\omega)}{\tan(n\pi/2)} = \Gamma(1-n)\cos\left(\frac{n\pi}{2}\right) S\omega^n \tag{7}$$

where $S$ is the gel strength (in Pa s$^n$) and $n$ is the gel index (or the gel exponent).

We can draw upon the idea that this power-law behavior is a summation of contributions from structural elements of varying length scales, and re-express the power law relaxation modulus over a finite range of time ($t_{\min} < t < t_{\max}$) as a summation of discrete relaxation modes with frequency response given by:

$$G'_{gel} = \frac{G_0}{2} + G_0 \sum_{k=1}^{K} \frac{(\lambda_k \omega)^2}{1+(\lambda_k \omega)^2}, \quad G''_{gel} = G_0 \sum_{k=1}^{K} \frac{(\lambda_k \omega)}{1+(\lambda_k \omega)^2} \tag{8}$$

where the time constants of the characteristic relaxation modes are bounded by the range of available data to $\lambda_1 \approx t_{\max}$, $\lambda_K \approx t_{\min}$ and are interconnected by a recursion relationship $\lambda_k = \lambda_1 k^{-1/n}$. To be consistent with the continuous power-law relaxation modulus of a critical gel the modulus scale for each relaxation mode is set by the expression:

$$G_0 = \frac{S}{n\Gamma(n)\lambda_1^n} \tag{9}$$

Under high frequency excitations ($\omega \geq 20$ rad s$^{-1}$), small amplitude oscillatory shearing tests on the the gel show that it also exhibits an additional Rouse-like relaxation regime reflecting the linear viscoelastic response of individual network segments between the crosslinks [Winter and

Mours (1997)]. The additional contributions to the dynamic moduli in this regime can be expressed as a Rouse spectrum:

$$G'_R = G_R \sum_{k=1}^{\infty} \frac{(\lambda_k \omega)^2}{1+(\lambda_k \omega)^2}, \qquad G''_R = G_R \sum_{k=1}^{\infty} \frac{(\lambda_k \omega)}{1+(\lambda_k \omega)^2} \tag{10}$$

where $\lambda_k = \lambda_R / k^2$, and $\lambda_R$, $G_R$ are the relaxation time and modulus of the Rouse segments.

Therefore, in general, we can write the complete linear viscoelastic response of the gluten gel as:

$$\begin{aligned} G'(\omega) &= G'_{gel}(\omega) + G'_R(\omega) \\ G''(\omega) &= G''_{gel}(\omega) + G''_R(\omega) \end{aligned} \tag{11}$$

The dynamic moduli obtained from small amplitude controlled stress experiments at stress amplitude of $\sigma_0 = 50$ Pa are plotted in Figure 2. The experimental data are in excellent agreement with equation (7) to (11) and the linear viscoelastic parameters ($S$ = 1300 ± 100 Pa, $n$ = 0.17, $G_R$ = 803 Pa, $\lambda_R$ = 0.05s) are consistent with data obtained through other small strain measurements such as step strain relaxation and creep [Ng and McKinley (2008)]. From the Rouse relaxation modulus, we can estimate the segment length between junction points in the gluten network to be $l \sim (k_B T / G_R)^{1/3} \approx 20\,\text{nm}$.

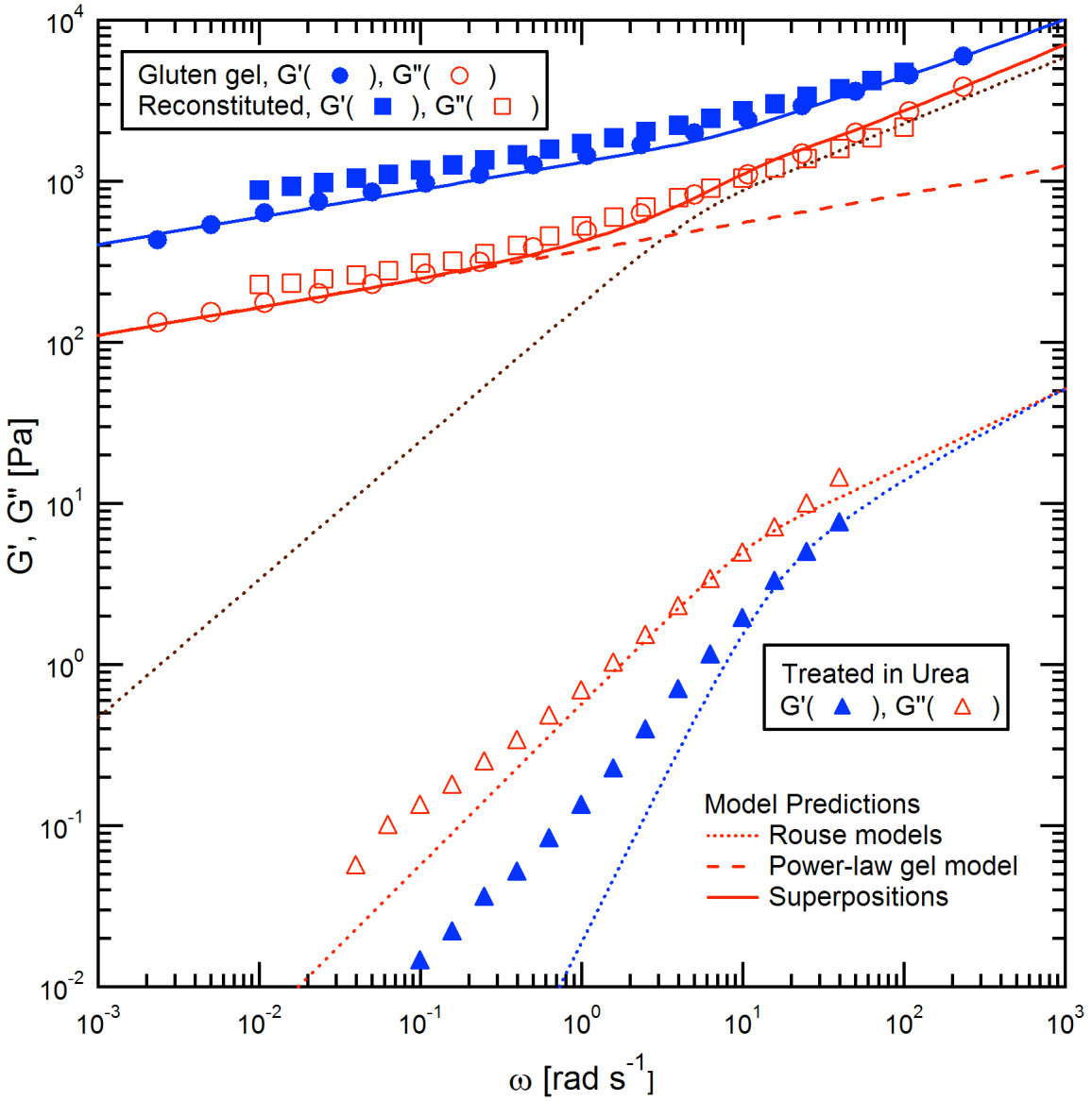


Figure 2 Storage and loss moduli of a gluten gel measured in small amplitude oscillation (circles) at T = 22° C. Solid lines represent predictions from equation (7) to (11), the superposition of power-law gel and Rouse models: $S = 1260$ Pa s$^n$, $n = 0.17$, $G_R = 803$ Pa, $\lambda_R = 0.05$ s. The response of a gluten gel dissolved in 8M Urea solution (triangles) and the corresponding reconstituted dough (squares) are also shown. The dissolved gluten shows a viscoelastic fluid-like behavior with significantly lower moduli. The gluten gel that is reformed by diluting the solution with water to wash out the Urea is almost identical to the original sample.

Figure 2 also illustrates the strong but reversible physico-chemical nature of the cross-links in a gluten gel. Although the gel network is formed by hydration in water, it is not soluble in water: introducing more water during the process of mixing does not "dilute" the gel, instead the excess water forms a pool at the bottom of the mixing bowl [Ng and McKinley (2008)]. However, it is possible to disrupt the network structure formed by the glutenin chains by diluting the gluten gel in 8M Urea solution (5 g gluten in 35 ml of 8M Urea solution). The resulting mixture exhibits the characteristic response of a weakly viscoelastic liquid with dramatically reduced storage and loss moduli. Draining this solution through a 30 μm sieve leaves no significant residues. The diluted solution still shows a Rouse-like viscoelastic response characteristic of a semi-dilute or concentrated solution (model shown for $\lambda_R = 0.05\,\mathrm{s}$, $G_R = 6.1\,\mathrm{Pa}$ in Figure 2 for sample treated in urea). Furthermore, the screening effect of the Urea is reversible. If the mixture is poured into a large beaker of water, filaments will appear which coagulate rapidly into a gluten dough. The linear viscoelastic properties of the gel harvested from this reformation process are also plotted in Figure 2. The gel shows a complete recovery to the original values of the moduli indicating the physical interactions at junction points are reversibly disrupted by the presence of Urea.

These observations suggest that the original gel network is predominantly held together by temporary physical interactions at junction points such as hydrogen bonds or possibly hydrophobic interactions [Creeth (1978); Zou *et al.* (1998)], while the macromolecular backbone of the glutenin chains is not significantly affected by the Urea treatment. They are also consistent with the proposed structural model of Letang *et al.* (1999); the hydrogen bonds or hydrophobic interactions allow the individual structural elements (composed of gluten molecules) to percolate and form a sample-spanning network structure which is consistent with the critical gel model.

We can highlight some general features of gluten gels and many other biopolymer networks by comparing and contrasting the results from this set of experiments to a familiar substance: vulcanized rubber consisting of polymer strands that have been cross-linked at network junctions [Treloar (2005)]. Due to the permanence of the covalent cross-links, rubbers display strong elasticity with little dissipation. However, beyond a typical yield strain or stress, the *intra-molecular* bonds within the macromolecular strands can rupture, causing the network to be irreversibly damaged; this event is manifested macroscopically as a progressive strain-softening and ultimately cohesive failure. In the case of gluten gels, these permanent cross-links are replaced by hydrogen bonds and hydrophobic interactions between chains. Since the strength of these junctions are typically weaker than those in covalent bonds, the tensile force accumulated under large strains within the polymer strands can be released by yielding of these *inter-molecular* junction points, thus avoiding irreversible rupture of the network segments. Furthermore, these transient junction points have the potential to reform if the material is returned to a state of lower stress, allowing the network to regain its original gel strength. Similar responses can be seen in other aqueous polymeric gels including associative polymer solutions, mucin gels, and actin gels.

As an alternate approach to disrupting the junction point interactions through chemical means, we can also explore the dynamics of reforming and breaking these bonds through mechanical methods, i.e. through the application of large stresses and strains. We expect a decrease in the modulus of the material as the applied strain is increased because the tensile force carried by individual network segments will increase with strain, leading to a greater probability of breakage [Evans and Ritchie (1999)]. This phenomenon has already been observed in gluten gels and results in the strain-softening reported by Uthayakumaran *et al.* (2002). We seek to

model and quantify such observations within the context of the power law critical-gel model and the microstructural changes described above.

However, to this point, we have only presented data on the linear viscoelastic response of the gluten gel; for the controlled stress tests shown in Figure 2, the strain amplitude of the imposed oscillation was largest ( $\gamma_0 = 0.125$ ) for the lowest frequency data $\omega = 0.003$ s$^{-1}$, and is still well within the linear regime of the gluten gel at this frequency.

Under these linear viscoelastic conditions, the output signal (strain in this case) is sinusoidal; the two dynamic moduli *G'* and *G"* are clearly defined as the in-phase and out-of-phase component with respect to the input signal. The linear viscoelastic moduli are independent of strain amplitude and the corresponding Lissajous figures [Philippoff (1966); Tee and Dealy (1975)] are found to be elliptical for all frequencies. For nonlinear viscoelastic materials such as polymer melts and gels, the simple linear decomposition of the data is insufficient as the strain is increased because the periodic output signal deviates from a purely sinusoidal form [Cho *et al.* (2005); Ewoldt *et al.* (2008); Philippoff (1966); Tee and Dealy (1975); Wilhelm (2002)]. Measuring the systematic deviation from the linear response can be viewed as a technique for highlighting the key distinguishing features of a given material, especially if one possesses a language or framework for quantitatively describing this rheological fingerprint. The modeling and quantification of these non-linear features for gluten gels will be the subject of the following sections.

## V NON-LINEAR DEFORMATION OF GLUTEN GEL

In this section, we first describe and quantify the key rheological features exhibited by a gluten gel under large amplitude oscillatory shear (LAOS). We then construct a constitutive model

based on the network structure of the gel and demonstrate how this formulation is able to describe quantitatively a range of non-linear rheological phenomena observed in physically-crosslinked biopolymer gels.

## A. Large Amplitude Oscillatory Shear

In contrast to linear viscoelastic experiments, for large amplitude oscillations the material parameters are formally treated as functions of both the oscillation frequency and strain amplitude rather than just frequency alone [Dealy and Wissbrun (1990)]. The most common form of expressing this material response is through the use of Fourier decomposition [Wilhelm (2002)] For imposed deformation $\gamma(t) = \gamma_0 \sin \omega t$, the departure from a linear (sinusoidal) stress response at a given frequency and strain amplitude is contained in the higher Fourier harmonics:

$$\frac{\sigma}{\gamma_0} = \sum_{n=1}^{N} G_n'(\omega, \gamma_0)\sin(n\omega t) + G_n''(\omega, \gamma_0)\cos(n\omega t) \qquad (12)$$

where $G_n'$ and $G_n''$ represent, respectively, the elastic and viscous contribution to the stress response at a given frequency $\omega$ and amplitude $\gamma_0$. In the linear viscoelastic domain ($\gamma_0 \to 0$), we require the contribution from these higher harmonics to tend to zero such that the simple sinusoidal response is recovered.

$$\left.\frac{\sigma}{\gamma_0}\right|_{\gamma_0 \to 0} = G_1'(\omega)\sin(\omega t) + G_1''(\omega)\cos(\omega t) \qquad (13)$$

In this framework, each experiment can be thought of as probing the material response at a particular point in a two-dimensional parameter space with frequency $\omega$ on one axis and strain amplitude $\gamma_0$ on the other. This representation is often referred to as a Pipkin diagram [Pipkin

(1972)]. Ewoldt *et al.* (2008) have recently described a systematic language and framework for analyzing nonlinear rheological behavior in this Pipkin space, and we will adopt this framework here.

The characteristic shapes of these Lissajous figures for a gluten gel undergoing LAOS deformation over a range of strain amplitudes ($0.02 < \gamma_0 < 6.0$) at $\omega$ = 1.0 $s^{-1}$ are plotted in Figure 3. At small strains ($\gamma_0 < 1$), the Lissajous figures are essentially elliptical and therefore the material response is consistent with the linear viscoelastic model described by Equations (7) through (11). The shapes of the ellipses and the values of the viscoelastic moduli are only a function of frequency and are independent of strain amplitude. Equation (13) can be rewritten to eliminate the explicit time dependence by substituting the identities $\sin(\omega t) = \gamma/\gamma_0$ and $\cos^2(\omega t) = 1 - \sin^2(\omega t)$, to give

$$\sigma^2 - 2\sigma\gamma G' + \gamma^2\left(G'^2 + G''^2\right) = G''^2\gamma_0^2 \qquad (14)$$

where the magnitude of the complex modulus is $\left|G^*\right| = G'^2 + G''^2$. For any frequency $\omega$, this equation describes an ellipse with major and minor axis centered at the origin and enclosed area $\oint \sigma\, d\gamma = \pi\gamma_0^2 G''$.

As the strain amplitude is increased, the material response and shape of the Lissajous curves shown in Figure 3 deviate significantly from this simple behavior. A number of visually distinctive features can be observed: Firstly a gradual "softening" of the material is indicated by the clockwise rotation of the major axis towards the strain-axis. Secondly, a distinct "stiffening," indicated by the upturn of the shear stress, is observed at large strains. The magnitude of the enclosed area also increases with increasing frequency, indicating an increasingly dissipative

response [Dealy and Wissbrun (1990)]. It is evident that this wealth of non-linear features cannot be fully captured by simply reporting the dynamic moduli $G'(\omega)$ and $G''(\omega)$ familiar from linear viscoelasticity. To illustrate this, we plot three different measures of the elastic moduli as a function of strain in Figure 4.

The parameters $G_1'$ and $G_3'$ are the first and third in-phase (real) Fourier coefficient of the output signal (from equation (12)). The first harmonic coefficient $G_1'(\omega)$ represents the typical method of calculating storage moduli employed by rheometer software. For strain sweep experiments, frequently only the values $G_1'$ and $G_1''$ are reported, this is often justified by the fact that the higher harmonics are small [Smith *et al.* (1970); Wyss *et al.* (2007)] for example $G_3'$ is less than 12% in this case. But simply inspecting the relative magnitude of the first and third harmonic coefficient will not reveal the dramatic changes in the shape of the Lissajous curves observed at large strains in Figure 3. The Chebyshev decomposition outlined by Ewoldt *et al.* (2008) shows that even small numerical values of computed quantities such as $G_3'$ can represent

substantial nonlinearities in the stress decomposition because of the numerical front factors (typically with values of ¼ or smaller) that arise from the orthogonality relationships between different harmonic modes.

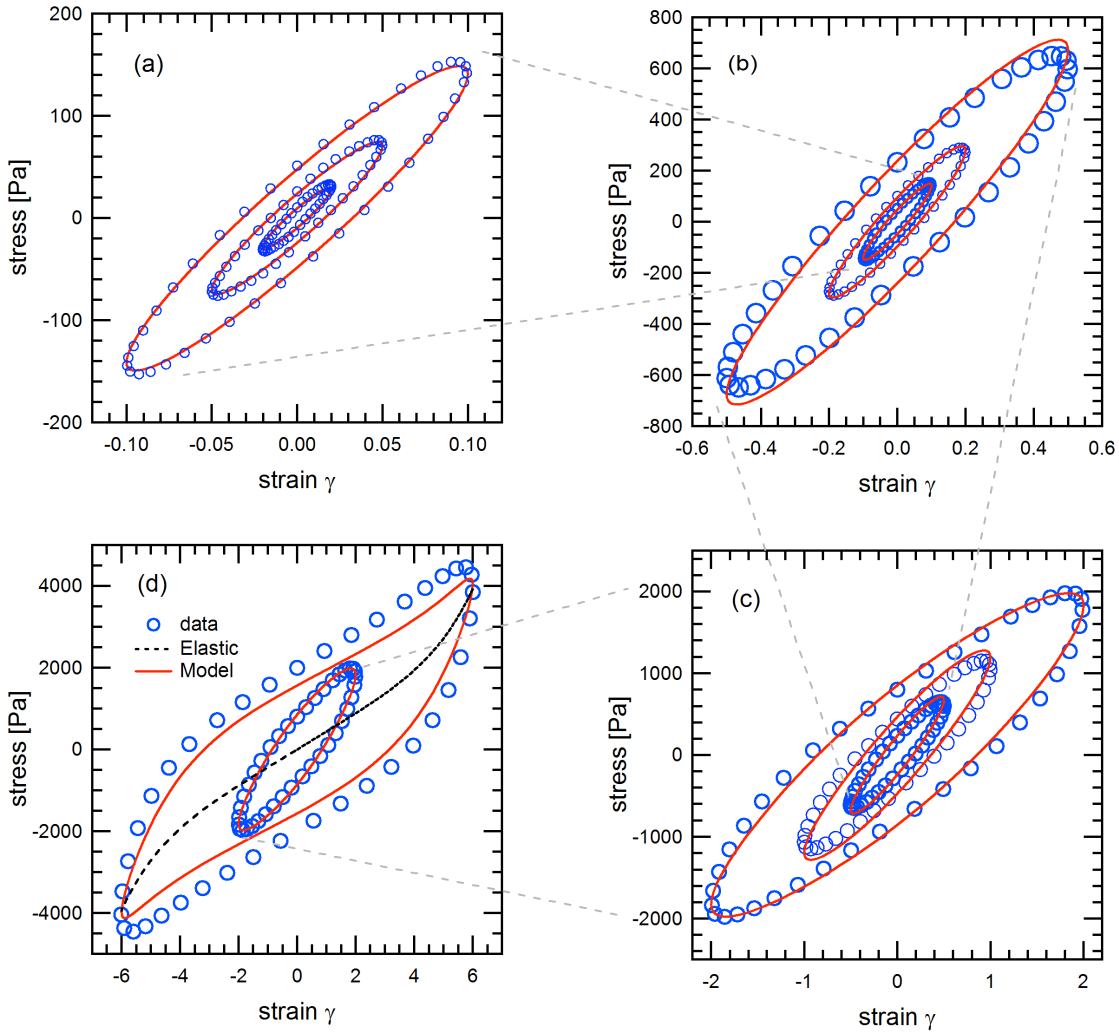


Figure 3 Lissajous-Bowditch curves after 12 oscillatory cycles for a gluten gel at fixed frequency $\omega = 1.0\ s^{-1}$ with (a) $\gamma_0 =$ 0.02, 0.05, 0.10, (b) $\gamma_0 =$ 0.10, 0.20, 0.50, (c) $\gamma_0 =$ 0.50, 1.00, 2.00, (d) $\gamma_0 =$ 2.0 and 6.00. As the imposed strain amplitude $\gamma_0$ increases from (a) to (d), the magnitude of the maximum stress grows and the axes are rescaled. Experimental data are plotted as open symbols. The decomposed elastic stresses are shown in the lower panel as a dotted line for $\gamma_0 = 6$. Predictions from the nonlinear generalized gel model described in the text are plotted as a solid line for each strain amplitude.

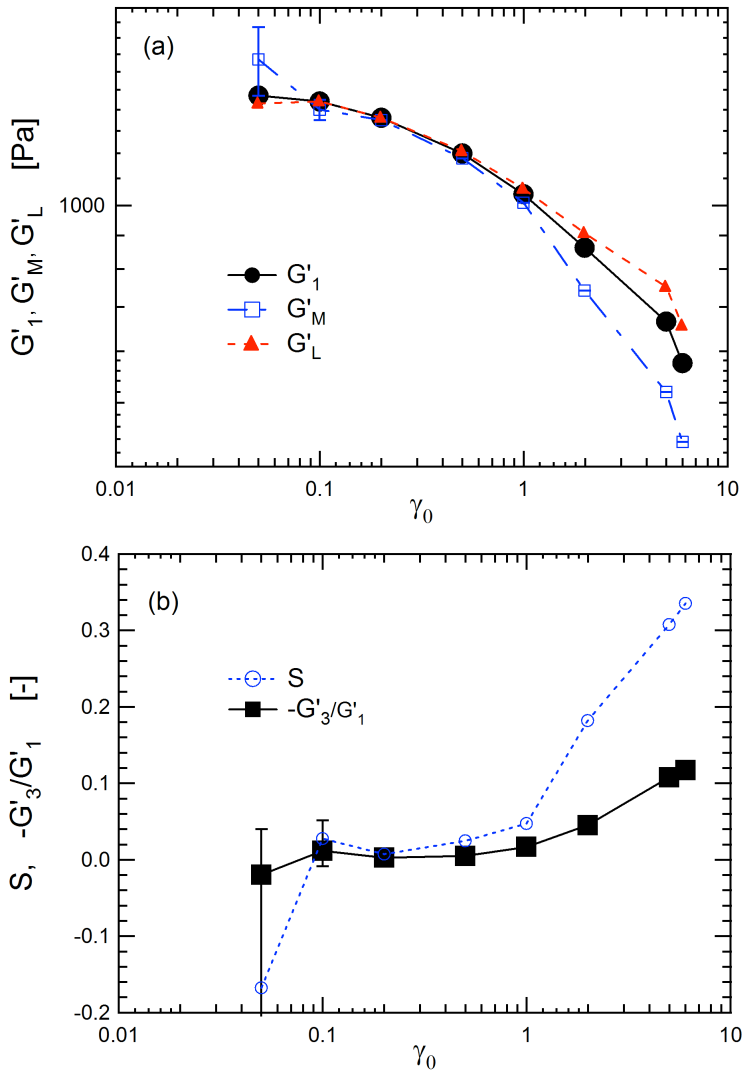


Figure 4 Dynamic moduli of gluten gel undergoing a strain-sweep (ARES rheometer, controlled strain mode) at $\omega = 1.0\ \mathrm{s}^{-1}$. The elastic modulus $G_1'$ and $G_3'$ are the first and third in-phase Fourier coefficient of the output signal, $G_1'$ is typically quoted as the "storage modulus"; $G_M'$ and $G_L'$ are the small and large strain moduli respectively, see equations (15), (16) and $S$ is the stiffening ratio defined in equation (19).

Instead, we use the geometrically-based definitions proposed by Ewoldt *et al.* (2008) as a simple yet practical method of quantifying these features in the Lissajous curves. In that work, the authors describe a number of complimentary definitions of relevant elastic moduli: $G'_M$ is the small strain dynamic modulus, which can be defined as the slope of the elastic Lissajous curve as it crosses through zero strain,

$$G'_M = \left.\frac{\partial\sigma}{\partial\gamma}\right|_{\gamma=0}. \tag{15}$$

Similarly, $G'_L$ is the large strain modulus and is defined as the secant or slope of the line connecting the origin to the stress measured at maximum strain,

$$G'_L = \left.\frac{\sigma}{\gamma_0}\right|_{\gamma=\gamma_0}. \tag{16}$$

In the linear viscoelastic regime, it can be shown that $G'_1$, $G'_M$ and $G'_L$ are all mathematically equivalent measures of the dynamic modulus by substituting these definitions (15)-(16) into equation (14). For $G'_L$ we calculate the stress at the maximum strain $\sigma_{\max}$:

$$\begin{aligned} \sigma_{\max}^2 - 2\sigma_{\max}\gamma_0 G' + \gamma_0^2\left(G'^2 + G''^2\right) &= G''^2\gamma_0^2 \\ \sigma_{\max} &= \gamma_0 G' \\ G_L' &= \frac{\sigma_{\max}}{\gamma_0} = G' \end{aligned} \tag{17}$$

And similarly, for $G'_M$ we calculate the rate of change of the stress with imposed strain by differentiating eq. (14) and evaluating it at $\gamma = 0$.

$$\frac{\partial}{\partial\gamma}\ [\sigma^2 - 2\sigma\gamma G' + \gamma^2\left(G'^2 + G''^2\right) = G''^2\gamma_0^2]\Big|_{\gamma=0}$$

$$2\frac{\partial\sigma}{\partial\gamma}\Big|_{\gamma=0} - 2G' = 0 \qquad (18)$$

$$G'_M = \frac{\partial\sigma}{\partial\gamma}\Big|_{\gamma=0} = G'$$

As the strain amplitude is increased, $G'_M$ does not remain constant, instead we see a gradual decrease in this measure of the small strain modulus which corresponds to the observed softening or clockwise rotation of the ellipse. The absolute value of $G'_L$ also decreases, however, this decrease is less "severe" compared to that observed in $G'_M$. These features can be interpreted jointly as the strain stiffening at large strains observed in the Lissajous figures and can be unambiguously parameterized by defining the following differential ratio between these two moduli.

$$S = \frac{G'_L - G'_M}{G'_L} \qquad (19)$$

The ratio *S* may be referred to as a stiffening ratio [Ewoldt *et al.* (2008)]. For an ideal linear viscoelastic system *S* = 0. A positive stiffening ratio implies stiffening of the viscoelastic network at large strains as observed in the Lissajous plots presented here.

Alternatively, we can visualize the elastic component by considering the method of decomposition described by Cho *et al.* (2005). This method utilizes symmetry arguments to define an elastic and viscous contribution to the shear stress that are purely odd (anti-symmetric) functions of strain and strain rate respectively:

$$\sigma = \sigma' + \sigma'' \qquad (20)$$

in which $\sigma'$ is the elastic contribution to the stress calculated through the following expression:

$$\sigma' = \frac{\sigma(\gamma, \dot{\gamma}/\omega) - \sigma(-\gamma, \dot{\gamma}/\omega)}{2} \tag{21}$$

where $\gamma = \gamma_0 \sin \omega t$ and $\dot{\gamma} = \gamma_0 \omega \cos \omega t$. The normalized elastic components are plotted in Figure 5.

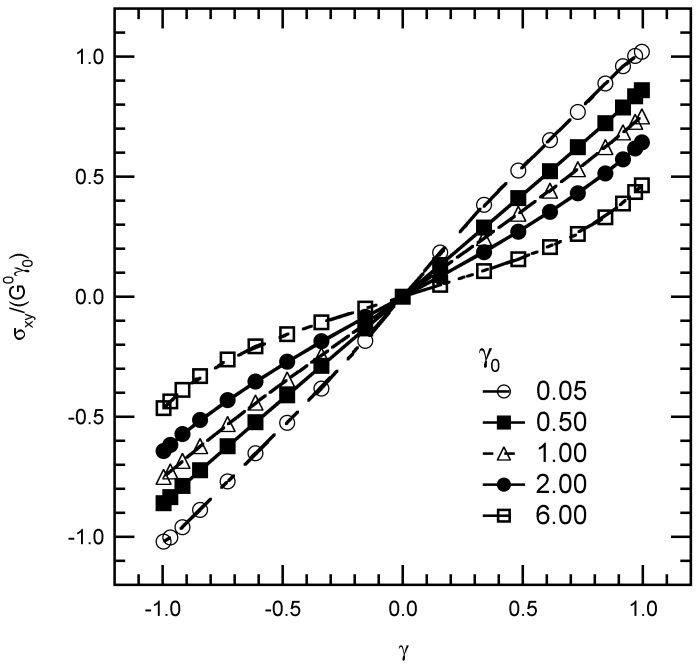


Figure 5 Normalized elastic stress extracted from the Lissajous curves for $\gamma_0$ = 0.03, 0.1, 0.3, 1.0, 3.0, 6.0 at $\omega = 1.0$ $s^{-1}$ and T = 22º C.

The normalized stress is calculated by dividing the stress by the "zero strain" modulus $G^0(\omega) = \lim_{\gamma_0 \to 0} G_1'(\omega, \gamma_0) = \lim_{\gamma_0 \to 0} G_M'(\omega, \gamma_0)$ and strain amplitude $\gamma_0$; the numerical value is calculated from small strain experiments at $\omega$ = 1 rad $s^{-1}$ and is found to be $G^0(1 \text{ rad s}^{-1}) \approx 1400 \text{ Pa}$ for this gluten gel. The clockwise rotation and non-linear stiffening of the elastic stress as the strain amplitude is increased are both clearly discerned using this technique.

The complete set of tests on the gluten gel can be compactly represented in the resulting rheological fingerprint shown in Figure 6. Each Lissajous curve represents the stress strain response over a single oscillation cycle at a specific set of coordinates $\{\omega, \gamma_0\}$ in the Pipkin space. The curves are shown after the initial transient response has decayed and reached a quasi-steady state, or in other words, these curves represent periodic attractors and the shapes are time invariant for successive cycles. Typically for gluten gels, this approach to a limit cycle requires a minimum of 4 periods of imposed deformation. We consider this initial transient decay or apparent thixotropic response further in Section V.D. Presenting the data in this manner gives a qualitative overview of the salient features over the range of strain amplitude and oscillation frequency as the material response transitions from the linear to non-linear regime.

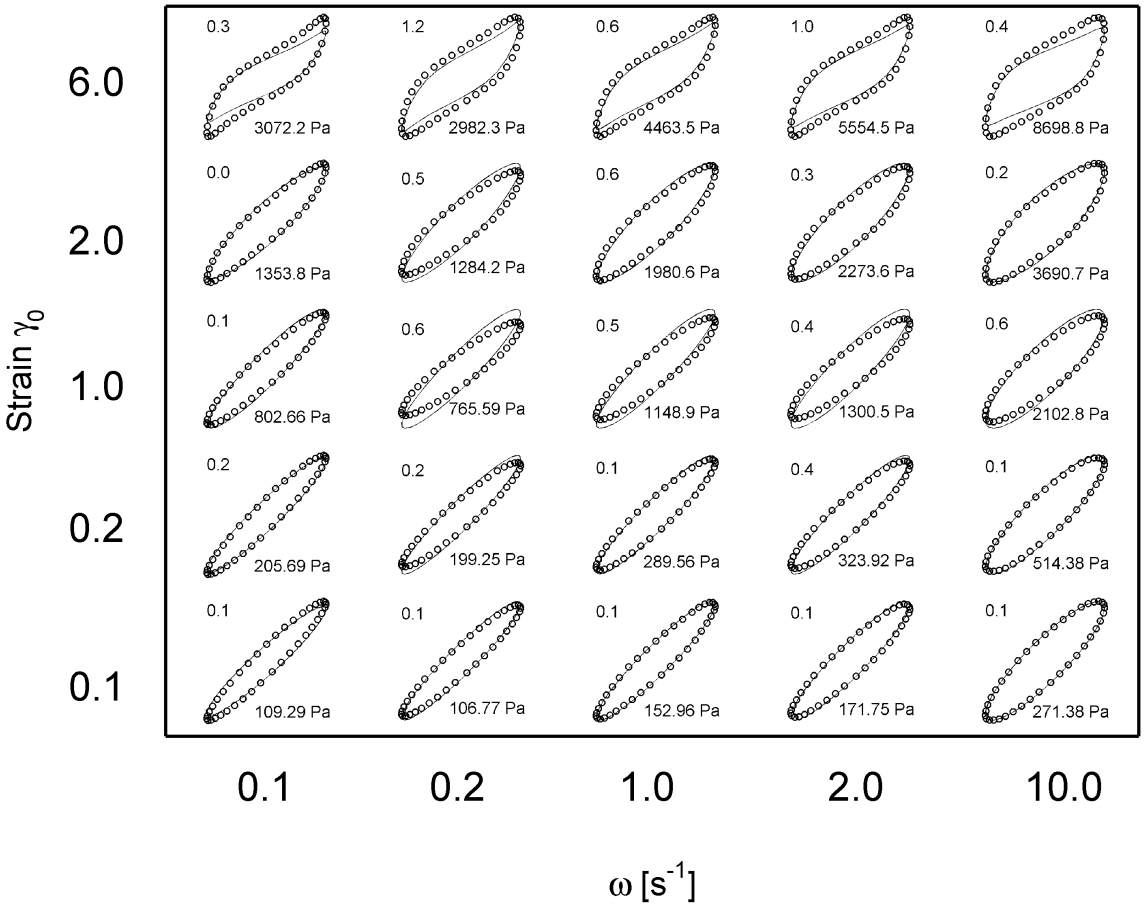


Figure 6. Rheological fingerprint of a gluten gel in Large Amplitude Oscillatory Shear (LAOS) flow. The shapes and maximum stress amplitude of each Lissajous curve is presented in a Pipkin space spanning $0.10 < \omega < 10\ \text{s}^{-1}$, $0.10 < \gamma_0 < 6.00$. In each case, the data represents the sixth cycle of the LAOS test and there are at least 80 experimental data points in each cycle. The relative error $\xi$ (defined in equation (33)) is given on the top left of each sub-figure, while the maximum stress associated with each limit cycle is displayed at the bottom right. The solid lines represent the predictions from the FENE network model discussed in section VB, equation (24).

## B. Network Model

We have described the non-linear features exhibited by a well-mixed gluten-water system under oscillatory shear qualitatively and introduced quantitative measures that highlight their magnitude and physical significance. In the following section, we consider how such features can be connected to the microstructural behavior of the gluten gel. A number of constitutive models with varying levels of complexities are available for doughs [Bagley *et al.* (1988); Charalambides *et al.* (2006); Phan-Thien *et al.* (1997); Ramkumar *et al.* (1996); Wang and Kokini (1995)]. In this article we select a level of complexity that is sufficient to explain the observed features, but yet simple enough so that we are not overwhelmed by a large number of equations containing an excessive number of material parameters to be fitted.

In our previous work [Ng and McKinley (2008)] and in section IV, we have shown that the rheology of gluten can be well represented in terms of the response of a transient nonlinear elastic network, and we therefore begin by modeling the gluten gel as a transient network of interacting filaments. The basic concepts underlying such network theories are succinctly outlined in Bird *et al.* (1987b), and the canonical LAOS responses of a prototypical network theory have been classified by Sim *et al.* (2003). The gel is idealized as an affinely deforming network and we refer to the filaments spanning junction points as elastic segments. These segments are assumed to have a distribution of end-to-end vectors $\mathbf{Q}_k$.

The contribution to the total stress tensor $\pi_k$ resulting from the distribution of chain stretch and orientation for each species *k* can be written as:

$$\pi_k = n_k H f\left(Q_k\right)\left\langle \mathbf{Q}_k \mathbf{Q}_k \right\rangle \tag{22}$$

Where $\langle \mathbf{Q}_k \mathbf{Q}_k \rangle$ is the ensemble average of the second order tensor $\mathbf{Q}_k \mathbf{Q}_k$, $n_k$ is the number density of the *kth* segments in the network, $H$ is the Hookean spring constant of an elastic segment and $f(Q_k)$ represents the non-linearity of the elastic restoring force as the stretch of the segment is increased. The transient nature of the network is reflected in a continuous dissociation of network junctions characterized by a rate of destruction $\lambda^{-1}(\mathbf{Q}_k)$, and a rebirth of junctions that are in the equilibrium state at a constant rate $L_k$. Hence the evolution equation of the second order tensor $\langle \mathbf{Q}_k \mathbf{Q}_k \rangle$ can be written in the following way:

$$\langle \mathbf{Q}_k \mathbf{Q}_k \rangle_{(1)} = L_k Q_{k,eq}^2 \mathbf{I} - \frac{\langle \mathbf{Q}_k \mathbf{Q}_k \rangle}{\lambda(\mathbf{Q}_k)} \tag{23}$$

where $Q_{k,eq}^2 = Tr\langle \mathbf{Q}_k \mathbf{Q}_k \rangle_{eq}$ is the mean square length of the segment at equilibrium and the subscript (1) indicates the usual upper convected derivative.

Equations (22) and (23) can also be expressed in terms of the dimensionless microstructural tensor $\mathbf{A}_k$

$$\begin{aligned} \pi_k &= G_k \left[ f(\mathbf{A}_k) \mathbf{A}_k \right] \\ \mathbf{A}_{k(1)} &= L_k \mathbf{I} - \frac{\mathbf{A}_k}{\lambda(\mathbf{A}_k)} \end{aligned} \tag{24}$$

where $\mathbf{A}_k = \langle \mathbf{Q}_k \mathbf{Q}_k \rangle / Q_{k,eq}^2$ and $G_k = n_k H Q_{k,eq}^2$ is the contribution of the $k$ segments to the elastic modulus of the transient network.

To capture the stiffening effect observed in our experiments, we consider a commonly used non-linear spring law [Bird (2007); Bird *et al.* (1987b); van den Brule (1993)] of the *FENE-P* form:

$$f\left(\mathbf{A}_k\right)=\frac{1}{1-Tr\left(\mathbf{A}_k\right)/b} \tag{25}$$

where $Tr\left(\mathbf{A}_k\right)=A_{k,11}+A_{k,22}+A_{k,33}$ denotes the trace operator and $b$ is the FENE parameter that characterizes the limit of extensibility of the polymeric strand. The functional form of equation (25) is illustrated in Figure 7(b). Other nonlinear spring laws with additional parameters have also been used to describe the finite extensibility in an elastic network [Evans and Ritchie (1999); Janmey (1991); Storm *et al.* (2005)] but will not be considered further here.

Next we turn our attention to the term describing the rate of destruction ($\lambda_k^{-1}$) of elastic segments. For the transient network at equilibrium, the rate of creation of network junctions has to be exactly balanced by the rate of destruction (by definition of equilibrium). However, under increasing deformation, as individual filaments become increasingly stretched, the probability of them detaching from the network increases and thus the corresponding rate of destruction should also increase. In effect, the average magnitude of the second moment tensor $\left\langle \mathbf{Q}_k\mathbf{Q}_k \right\rangle$ is reduced with increasing deformation amplitudes, leading to a softening that is manifested in the Lissajous figures as an apparent clockwise rotation of the major axis of the ellipse. We model this effect by assuming an empirical first order network destruction rate that is a function of the magnitude of the microstructural stretch $\mathbf{A}_k$:

$$\lambda_k^{-1}=\lambda_{k,eq}^{-1}\left(1+C_1\left[Tr\left(\mathbf{A}_k\right)-3\right]\right) \tag{26}$$

where $C_1$ is a constant to be determined that characterizes this increased rate of network breakage. The scalar parameter $\lambda_{k,eq}$ is the linear viscoelastic relaxation time, i.e. the

characteristic structural relaxation time in the limit of infinitesimal microstructural deformation ($Tr\left(\mathbf{A}_k\right)\to 3$).

Furthermore, we require the rate of network destruction to become increasingly rapid as the tension in the network filaments diverges near the finite extensibility limit (in that $Tr\left(\mathbf{A}_k\right)\to b$). Once more, we express this as a FENE like term:

$$\lambda_k^{-1}\sim\frac{1}{1-Tr\left(\mathbf{A}_k\right)/b} \tag{27}$$

We combine equations (26) and (27) to write a non-linear rate of network destruction that captures these two physical ideas:

$$\lambda_k^{-1}\left(\mathbf{A}_k\right)=\lambda_{k,0}^{-1}\frac{1+C_1(Tr\left(\mathbf{A}_k\right)-3)}{1-Tr\left(\mathbf{A}_k\right)/b} \tag{28}$$

The corresponding rate of creation required to maintain steady state at equilibrium conditions ($\mathbf{A}_{k,eq}=\mathbf{I}$) is then:

$$L_k=\lambda_{k,0}^{-1}\frac{1}{\left(1-3/b\right)}=\lambda_{k,eq}^{-1} \tag{29}$$

The deviatoric stress tensor $\sigma_k$ can then be written as:

$$\begin{aligned}\sigma_k&=\pi_k-p\mathbf{I}\\&=\pi_k-\pi_{eq}\\&=G\left(f\left(\mathbf{A}_k\right)\mathbf{A}_k-f_{eq}\mathbf{I}\right)\end{aligned} \tag{30}$$

where $Gf_{eq}=G\left(1-3/b\right)^{-1}$ is the equilibrium contribution of this mode to the isotropic stress or elastic 'pressure' in the gel.

Various techniques for obtaining the linear viscoelastic parameters that characterize these relaxation modes were outlined by Ng and McKinley (2008). Here, we extend this idea to the nonlinear regime and represent the response as a series of non-linear network modes each of the form equation (30) such that

$$\sigma = \sum_{k}^{K} \sigma_k \ . \tag{31}$$

In this form, the network model will give linear viscoelastic response that is identical to equation (7) through (11) and yet still allow for the non-linear features to become apparent at large strains.

We summarize the construction of this model in Figure 7. The linear viscoelastic parameters of the model, $S$ =1400 Pa s$^n$, $n$ = 0.175, $G_R$ = 803 Pa and $\lambda_R$ = 0.05 s, are obtained by fitting equations (7) through (11) to the small amplitude oscillatory shear (SAOS) data or other equivalent linear viscoelastic measurements. The gel parameters $S$ and $n$ are then combined to generate a series of discrete modal relaxation times $\lambda_k = \lambda_1 k^{-1/n}$ with zeroth order modulus $G_0 = S \big/ \left( n\Gamma(n)\lambda_1^n \right)$; here $\lambda_1$ is an arbitrarily chosen maximum time scale, $\lambda_1 = 10^4$ s, and $K$ (taken here to be $K$=30) is the total number of gel modes to span the relevant time scale. This conversion is illustrated in Figure 7a. This series of gel modes, $G_{gel}(t) = \frac{G_0}{2} + G_0 \sum_{k=1}^{K} \exp\left(-t/\lambda_k\right)$, together with the Rouse modes, $G_{Rouse}(t) = G_R \sum_{m=1}^{M} \exp\left(-tm^2/\lambda_R\right)$, capture the entire relaxation spectrum of the gluten gel and provides an excellent approximation to the powerlaw relaxation function $G(t) = St^{-n}$.

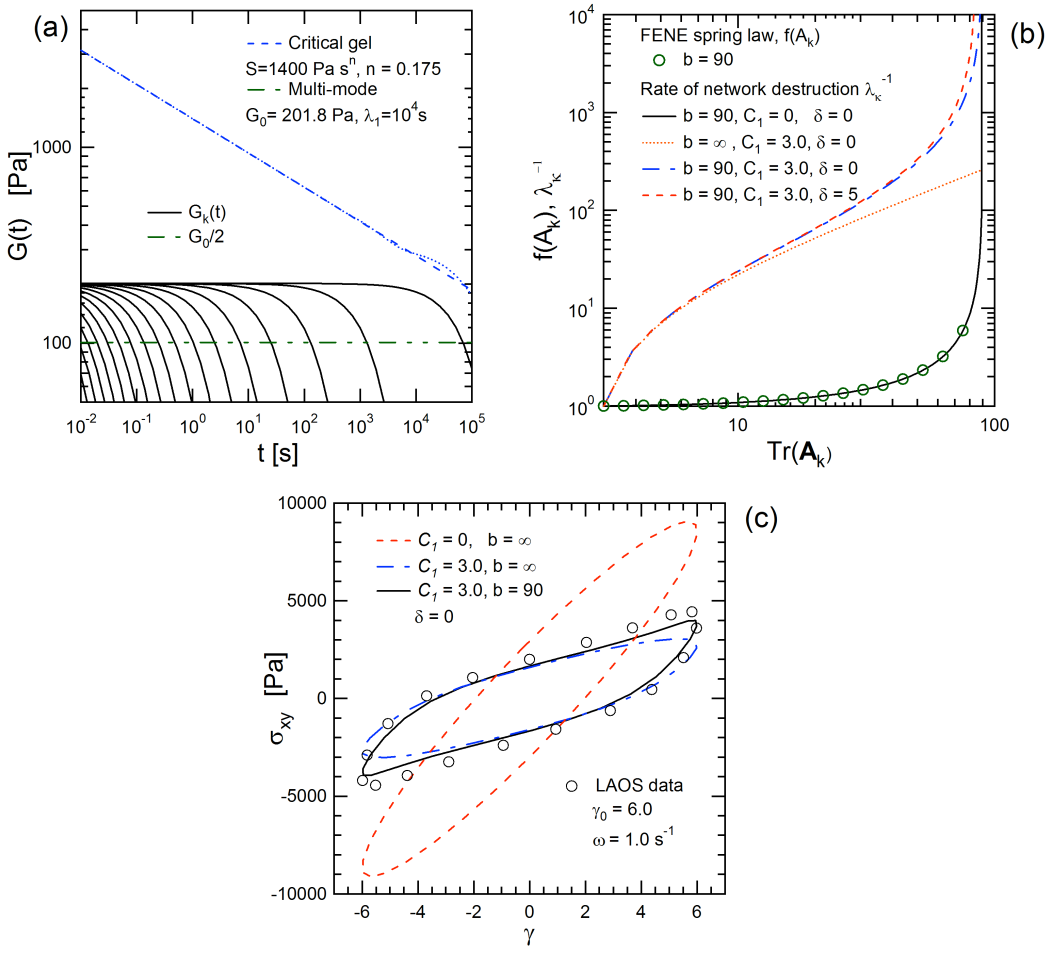


Figure 7. Summary of constitutive parameters in the FENE network model.

(a) The critical gel-like behavior observed in linear viscoelastic tests is approximated by a series of Maxwell relaxation modes; $G_{gel}(t) = St^{-n} \simeq G_0/2 + \sum G_k(t)$. The total relaxation modulus is given by $G(t) = G_{gel}(t) + G_R(t)$. (b) Non linear functions in the network model. A FENE type spring law is used as the non linear modulus $f(A_k)$ and is characterized by the finite extensibility limit $b$. The rate of junction destruction $\lambda_k^{-1}$, is characterized by two additional parameters; $C_1$ describes an increase in the network destruction rate at intermediate microstructural deformations; $\delta$ modifies the FENE function by allowing the junction points to be destroyed close to, but before, the finite extensibility limit $b$ is reached. (c) Lissajous figures for LAOS tests on a gluten dough at $\gamma_0 = 6$. The quasi-linear formulation with $C_1 = 0$ and $b \to \infty$ grossly over predicts the stress. Inclusion of the $C_1$ term gives strain softening (clockwise rotation of ellipse). A small degree of strain-stiffening is apparent at large strain when the non-linear FENE spring law is introduced.

Finally, we recall that the linear viscoelastic network response of the gluten gel in an arbitrary deformation can be represented as a summation of individual modes such that:

$$\sigma = \int_0^t G(t-t')\dot{\gamma}\, dt' = \sum_{k=1}^{K} \int_0^t G_{k,gel}(t-t')\dot{\gamma}\, dt' + \sum_{m=1}^{M} \int_0^t G_{m,R}(t-t')\dot{\gamma}\, dt' \qquad (32)$$

The numerical values of the two non-linear model parameters $C_1$ = 3.0 and $b$ = 90 are obtained by a manual fitting process to the large amplitude oscillatory shear (LAOS) data. For the sake of simplicity, the same values for $C_1$ and $b$ are used for all modes $1 \leq k \leq K$. The respective contributions from each of these non-linear parameters are illustrated in Figure 7 (c). This value of $b$ is within the range of typical reported values of finite extensibility ($10 < b < 1000$) [Bird *et al.* (1987b)] and corresponds to a stretching of the network segment through approximately 10 times its original length.

We now return to the Lissajous curves presented in Figure 3 and Figure 6, and compare the curves with the predictions of the FENE network model which are also plotted on the same figure. It is apparent that the network model is able to capture both the global rotation and local stiffening of the measured data with reasonable quantitative agreement. An estimate of the relative R.M.S. error is also given on the plot. The relative error $\xi(\omega,\gamma_0)$ is calculated from the set of $N$ data points for a given strain amplitude and frequency through the following definition:

$$\xi(\omega,\gamma_0) = \frac{1}{N}\sqrt{\sum_{n=1}^{N}\left(\frac{\sigma_{FENE}(n)-\sigma_{data}(n)}{\sigma_{data}(n)}\right)^2} \qquad (33)$$

The deviations between the model and data are most apparent at intermediate to large strains ($\gamma_0 > 1.00$). In general, the measured apparent stress is slightly larger than the model prediction.

This trend is consistent with the small systematic error expected from the inhomogeneous deformation of torsional parallel plate measurements (for a material that exhibits overall softening or thinning with increased deformation). In the nonlinear regime the inhomogeneous deformation field makes calculation of the true stress for a large-amplitude time-varying deformation imprecise. Expressions for calculating the true rim stress for solid-like materials can be found in Phan-Thien *et al.* (2000). See the supplementary material at [URL will be inserted by AIP] for a detailed discussion of the errors between apparent and true stresses, and a method for systematically and efficiently correcting experimental data.

In addition to the errors induced by measurement imprecision, the discrepancy between model and experiment may also arise from an over-simplification of the softening function used in equation (26). Further improvements to this function are discussed in Section VI.

## C. Frequency Dependence of Lissajous Figures

Returning once more to the rheological fingerprint for the gluten gel shown in Figure 6, we see that the qualitative effect of increasing strains are similar at all frequencies. As already noted in the figure and in equation (14), at small strains ( $\gamma_0 < 1$ ) the Lissajous curves are elliptical and the resulting frequency response is well predicted by either the integral power-law or differential multimode forms of the critical gel and Rouse spectrum presented in section IV or by the linear viscoelastic limit of the multi-mode FENE network model.

In Figure 8, we focus on the comparison between the network predictions and the measured Lissajous curves of varying frequencies at large strains ( $\gamma_0 \geq 1$ ). As the oscillatory frequency increases, the maximum shear stress attained in each cycle increases and the area enclosed by the

curve also increases; corresponding to an increasingly dissipative material response. The model provides a good qualitative agreement, the changes in shape and enclosed area of the Lissajous curves are captured by the network model while other salient features such as the clockwise rotation and local strain stiffening are also present in the predicted response. Further improvements to the quantitative accuracy of the model are discussed briefly in the conclusion section.

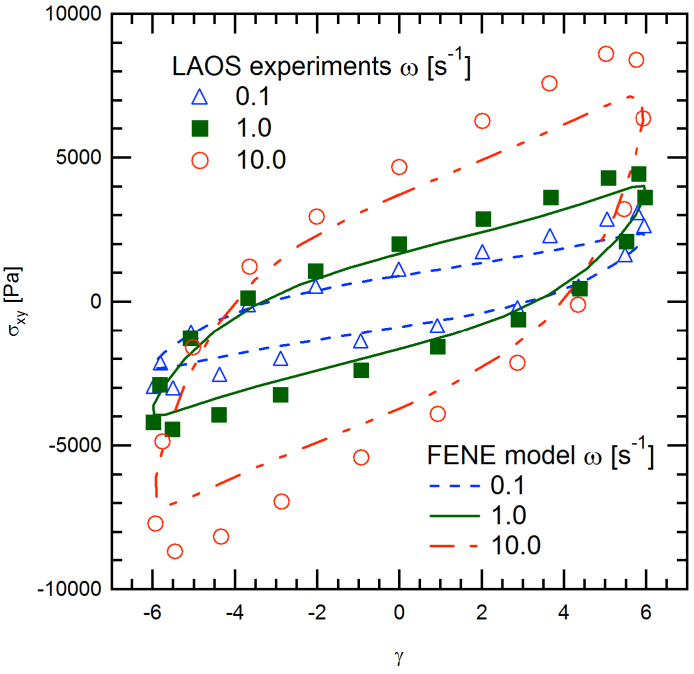


Figure 8 Lissajous curves of a gluten gel performed at large amplitude for a range of frequencies $\omega$ = 0.1, 1,0 and 10 $s^{-1}$ at $\gamma_0 = 6$. The FENE network model correctly predicts the trends and magnitude of stress over the frequency range probed.

## D. Transient Oscillatory Response

The presence of very long relaxation times (for example $\lambda_1 = 10^4$ s in Fig. 7) results in extended changes in the network structure of the critical gel as the equilibrium distribution of junctions break and reform following the inception of deformation; this gives rise to a form of thixotropic response. The transient behavior arising from these network changes is distinctly different from linear viscoelastic transients that involve infinitesimal changes to microstructure.

We illustrate the differences between small strain and large strain transient responses by considering a situation in which the imposed oscillatory strain amplitude is suddenly changed while we monitor the transient stress response. This is realized experimentally by changing the amplitude of oscillation from $\gamma_0 = 0.10$ to $\gamma_1 = 3.0$ at time $t_1$, and then back to $\gamma_0 = 0.10$ again.

The experimental transient stress response is plotted in Figure 9a and b. To scale out the large change in stress amplitude associated with the step change in strain, in Figure 9c we plot the transient modulus (or scaled stress) defined as:

$$G_A(t) = \frac{\sigma_{xy}(t)}{\gamma_0}$$
$$\gamma_0\{t\} = 3.0 \text{ for } 106.8 < t < 169.6 \text{ s} \qquad (34)$$
$$= 0.1 \text{ otherwise}$$

The experimental data for $t > t_1 = 106.8$ s clearly shows a pronounced transient decay during the first five cycles after the increase in oscillation amplitude. During this time the material progressively softens; as indicated by a decrease of the transient modulus by as much as ~40% (from 1300 Pa to 800 Pa). Quasi-linear or linear viscoelastic constitutive models of the form:

$$\sigma_{xy} = \int_0^t G(t-t')\gamma_0\omega\cos(\omega t)dt' \qquad (35)$$

will in fact predict an increasing stress amplitude that converges rapidly to the linear viscoelastic modulus with a response of the form $\sim(1-e^{-t/\lambda_1})$. The linear response is plotted in Figure 9c as a dotted line. The long transient softening or apparent thixotropic response is captured more accurately by the inclusion of the finite-extensibility and strain-dependent network destruction terms as shown by the solid line in Figure 9. These lines represent the response of the constitutive model given by equations (24) to (31). We emphasize that there are no adjustable parameters here; *S* and *n* are determined from linear viscoelastic experiments, the corresponding discrete spectrum for the linear response is given by equation (10). The nonlinear response is given by integrating equations (24) to (31) with $b = 90$, and $C_1 = 3.0$ (determined by fitting to the data in Figure 3). Furthermore, the predicted complete recovery to the small amplitude modulus

is also observed experimentally for times $t > t_2$ = 169.6s. This can be understood by analogy to the experiments conducted by reversibly "breaking" the network structure through dilution with Urea and the subsequent reconstitution by washing out the Urea with water (Figure 2). In large amplitude oscillations, the hydrogen bonds at network junctions are reversibly broken through mechanical loading and imposition of large strains on the network. Upon reduction of the imposed strain at $t_2$ = 169.6s, the reversible nature of the hydrogen bonding events means that the gel is able to reform its network structure. The oscillatory stress slowly decays over multiple cycles and relaxes back towards the elliptic limit cycle shown in Fig. 9(b). Neither mechanical nor chemical treatment has an effect on the covalent interactions within the filaments, thus allowing complete recovery of the network structure when the "disruptions" are removed. Such complete recovery contrasts with the irreversible rupture of covalent bonds in a chemical gel. The recovery of the gluten gel can also be contrasted with the incomplete recovery of wheat flour doughs, e.g. Hibberd and Wallace (1966), in which additional bonding interactions between the gluten chains and starch particles must be considered. These latter interactions can be described by damage functions [Tanner *et al.* (2008)] in which the network changes are permanent and irreversible.

## E. Comparison with other non-linear deformations

So far we have focused solely on the mechanical response under large amplitude oscillatory deformations, next we address briefly the rheological predictions of the finitely extensible network model in the start up of transient deformations. We first compare the model predictions to the transient growth in the shear stress during the start up of steady shear flow. The model and data show good agreement with experimental data in the power-law regime $\gamma^* \leq 5$ for which

$\sigma_{xy}^{+} \sim t^{n}$ and $N_1^{+} \sim t^{2n}$. In this regime, the predicted material response is also time-strain factorizable. Deviations from the power law growth and time-strain factorizability discussed in equation (5) are discernible when the strain-stiffening effect becomes significant. In fact the magnitude of the stress overshoot is grossly over predicted by the FENE network model. It is possible to reduce this apparent stress overshoot empirically by using an extremely non-linear elastic term [Phan-Thien *et al.* (1997)] that bounds the stress growth at very large strains. However, here we focus more on the causes of this apparent overshoot. Firstly, as discussed in our previous work [Ng and McKinley (2008)], video imaging shows that the sheared gluten sample begins to undergo an instability very rapidly after the onset of strain-stiffening ($\gamma^{*} \sim 5$). As the imposed strain continues to accumulate, this instability ultimately leads to the sample rolling up and being ejected from the gap. The deformation in the gluten gel is no longer viscometric from the point of instability onwards.

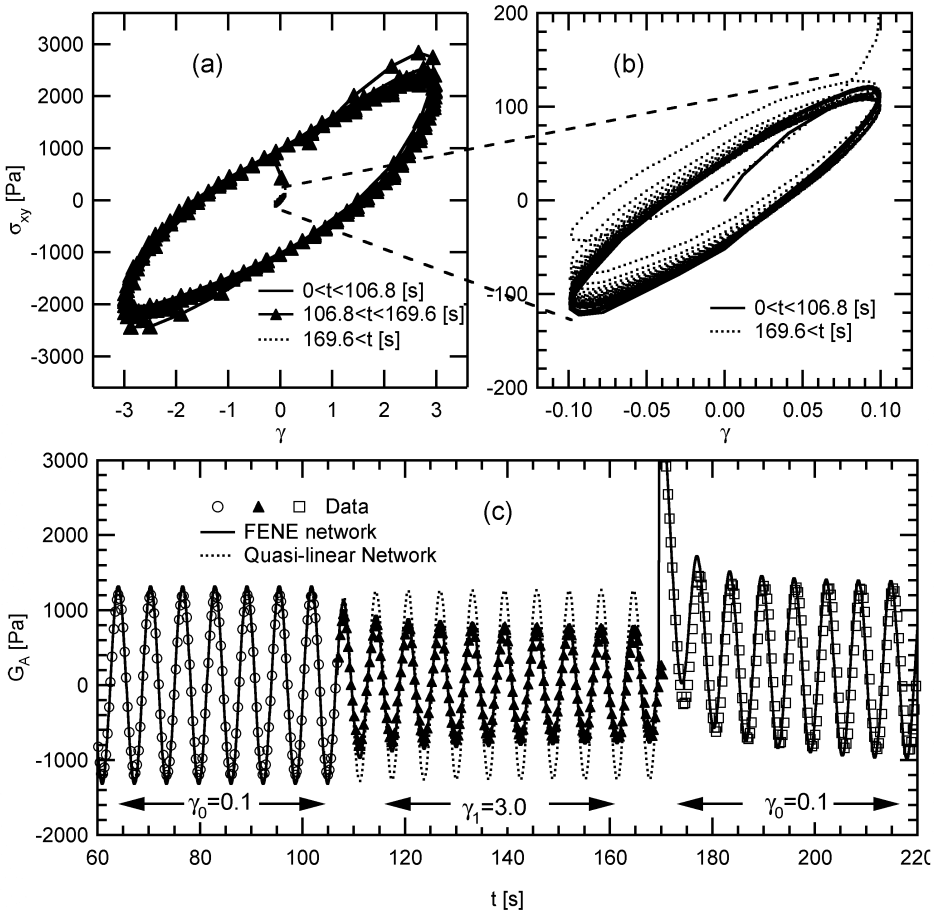


Figure 9 Transient behavior of gluten gel. (a). Lissajous figures depicting material response when the strain amplitude of oscillation is increased from $\gamma_0 = 0.10$ to $\gamma_0 = 3.0$, then back to $\gamma_0 = 0.10$ again at a fixed frequency of $\omega$ = 1.0 $s^{-1}$; (b) enlarged view of the approach back to the small strain limit cycle for $t > t_2$ = 169.6 s; (c) Temporal response of the scaled oscillatory stress or apparent modulus $G_A(t) = \sigma_{xy}(t)/\gamma_0$ illustrating the transient nature of the network. The FENE network correctly predicts the transient stress growth and complete recovery of the gluten gel when the strain amplitude is reduced.

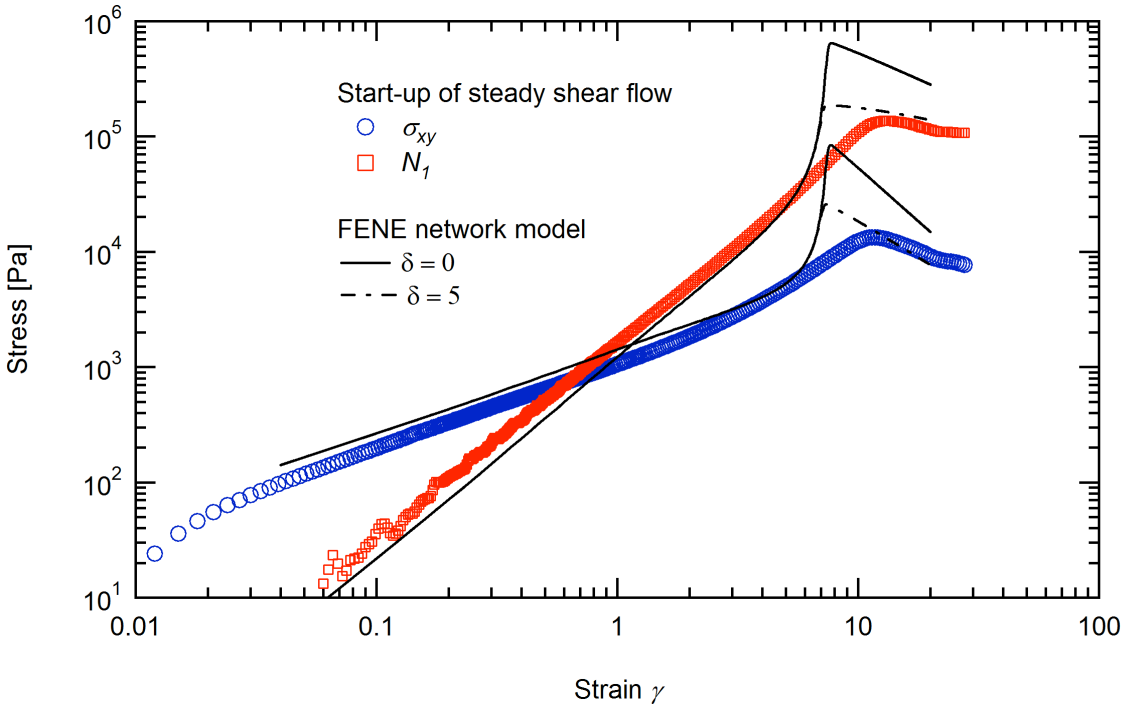


Figure 10 Start-up of steady shear flow at $\dot{\gamma}_0 = 1.0\ \mathrm{s}^{-1}$. The power-law growth in the shear stress and also in the normal stress difference is well predicted by the FENE network model up to $\gamma^* = 5$, after which the non-linearity of the model over predicts the measured over-shoot in the normal stress difference and the shear stress. Improvements to the predictions can be made by using the modified network model; however, accurate constitutive modeling at large strains is difficult because the sample deformation deviates substantially from viscometric flow at torsional strains $\gamma \sim 9$.

Secondly, we may also attribute part of this discrepancy once again to the simplified evolution equation. The proposed form of equation (27) captures the increased probability of the breaking of a junction point as the tension in the stretched filament is increased; however although this functional form is reasonable, there is no reason to suppose that the rate of breakage should only diverge when the chains reach the finite extensible limit (i.e. $Tr\left(\mathbf{A}_k\right) \to b$) The ultimate tensile strength supported by a junction point may be a finite value or, in other words, the probability of survival of a junction point should be able to tend to zero when a critical but finite value of

tension is sustained by a elastic segment. Therefore we consider a straightforward modification to the model by allowing the junctions to be completely destroyed slightly before the FENE limit. The modified rate of destruction can be written in the form

$$\lambda_k^{-1}\left(\mathbf{A}_k\right)=\lambda_{k,0}^{-1}\frac{1+C_1\left(Tr\left(\mathbf{A}_k\right)-3\right)}{1-Tr\left(\mathbf{A}_k\right)/\left(b-\delta\right)} \tag{36}$$

The resulting stress response of this modified network model is essentially the same as equation (27) through (31), but the stress overshoots are slightly tempered. In Figure 10 we show that the predicted magnitude of the overshoot is much more reasonable for the chosen value of $\delta = 5$.

Finally, the use of FENE-P type models with closure approximations are known to result in over-prediction of transient stress growth [Keunings (1997)]. The reason being that the Peterlin closure approximation cannot accurately capture the statistical distribution of segment lengths at intermediate deformations near the point of finite extensibility and instead predicts that a fraction of the filaments may be deformed beyond the maximum allowable length. More accurate simulations utilizing Brownian dynamics typically reveal a much weaker overshoot behavior [Ghosh *et al.* (2001)].

The constitutive model can also be used to predict the evolution of the stress in start-up of uniaxial extension flow as depicted in Figure 11. The data are collected on a wind-up drum type rheometer that has been discussed in detail in a previous publication [Ng and McKinley (2008)]. The quasilinear model predicts an initial power-law response with $(\sigma_{zz}-\sigma_{rr})\sim t^n$ before transitioning to an affine neo-Hookean response beyond a critical strain (for clarity, the quasi-linear response is shown only for $\dot{\varepsilon}_0 = 0.3\ \mathrm{s}^{-1}$ in Figure 11). The FENE network over-predicts the magnitude of the strain-hardening growth in the normal stress difference that occurs just before

the sample ruptures, while the modified network model gives more reasonable stress growth functions. The fact that the point of rupture occurs extremely close to the finite extensibility plateau should not be surprising, since the mass rupturing of network junctions dramatically reduces the rate of stress growth in the system and can lead to tearing or necking as implied in the Considère criterion [Considère (1885); Pearson and Connelly (1982); McKinley and Hassager (1999); Ng *et al.* (2006)].

Significantly, the maximum extensibility of dough is often quoted as a measure of its quality [Bloksma (1990b); Bloksma (1990a); Dobraszczyk (2004); Ewart (1989); Kokelaar *et al.* (1996); Sliwinski *et al.* (2004); van Vliet *et al.* (1992)], and this is the first piece of direct evidence that shows how the apparent extensibility (defined as the maximum strain achieved before rupture) of a dough can be linked to molecular phenomena, and be predicted or at least estimated by performing shear experiments at large oscillatory amplitudes: a reasonable estimate of the extensibility of a dough-like material can be inferred if the linear viscoelastic relaxation function $G\left(t-t'\right)=St^{-n}$ and the finite extensibility parameter $b$ are known. The magnitude of the stress may be over predicted by the bare FENE-P model (as shown in Figure 10) without additional experiments, but this does not affect the values of the critical strains.

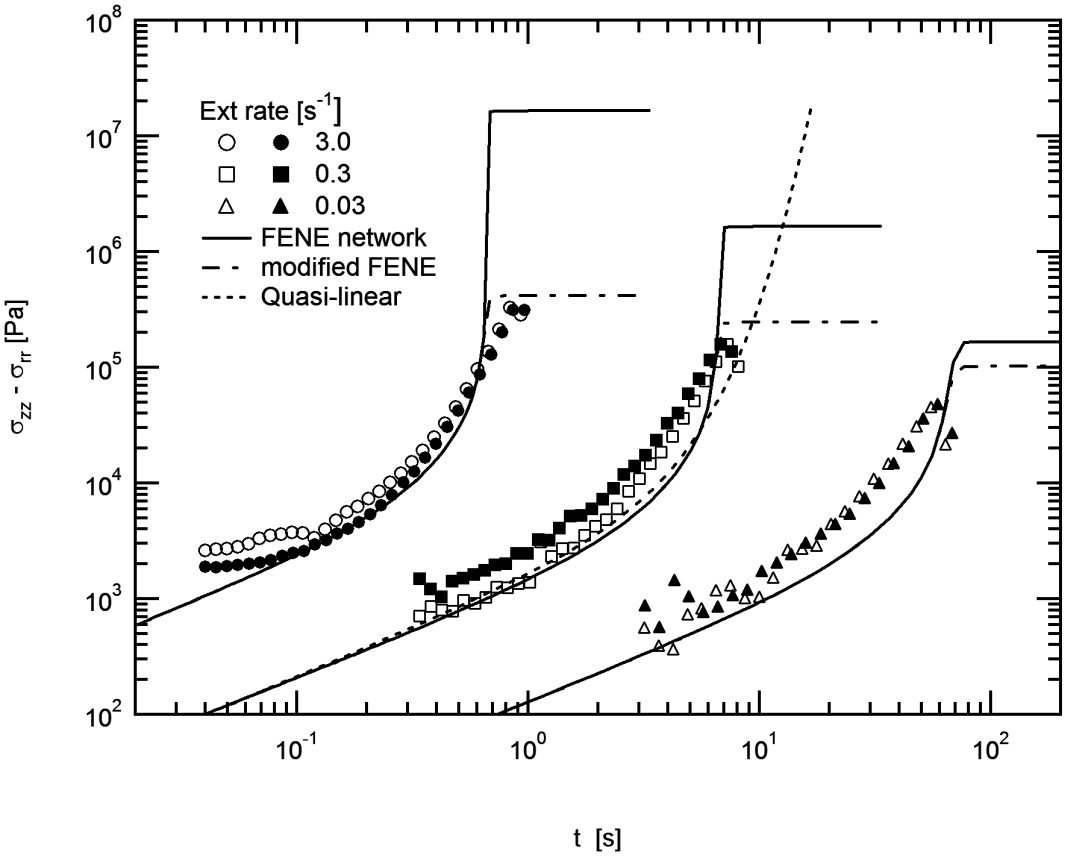


Figure 11 Transient extensional stress difference upon inception of uni-axial elongation for deformation rates $0.03 < \dot{\varepsilon}_0 < 3.0$ s$^{-1}$; experimental data is limited by sample rupture. Two experimental runs were performed at each strain rate to ensure reproducibility. The form of the quasi-linear simulation is shown for reference at $\dot{\varepsilon}_0 = 0.3$ s$^{-1}$. The FENE network over predicts the magnitude of stress, this can be remedied by a simple modification; see Eq.(36). The strain and time to rupture corresponds closely to that predicted by the finite extensibility limit determined from LAOS with $b = 90$ and $\delta = 5$.

## VI CONCLUSIONS

In this article, we investigated the mechanical properties of a gluten gel through large amplitude oscillatory shear (LAOS). This experimental technique allowed us to study the rheological response over a range of strain amplitudes $\gamma_0$ and frequencies $\omega$ with good accuracy and repeatability up to the point of viscometric instability without destruction of the sample. From the LAOS data, we are able to generate a rheological fingerprint of the gluten gel that in turn forms the basis for devising a constitutive equation capable of predicting the transient evolution of the stress in a range of nonlinear flows.

We have built upon the critical gel-like response documented in our earlier work to construct a constitutive model that captures the microscopic origin of the non-linear behavior in a gluten gel. The non-linearity of the constitutive equation is encapsulated in two simple functions, namely a FENE spring law that captures the strain-stiffening in the network and a non-linear network destruction term that reflects the observed softening behavior at intermediate strains. These two functions are coupled with two model parameters (*S, n*) that characterize the well-known power-law relaxation of a critical gel. We have demonstrated how this relatively low level of complexity in the constitutive model is sufficient to capture the important non-linear features observed in both transient shear and extensional deformations. Further improvements to the quantitative agreement between experiment and model can be made by fine tuning the forms of these non-linear functions and will be the subject of future work. We briefly describe some of the possible modifications here.

Perhaps most importantly, we have based our model on the multi-mode approach described in equation (8). Because of the frequency independence of the Lissajous fingerprint in Figure 6

and time-strain separability, we have assumed all the modes to have the same non-linear behavior (i.e. same values of the nonlinear model parameters $b$, $\delta$ and $C_1$) in order to minimize the number of adjustable model parameters. This allowed us to concentrate on the essential features of these non-linearities and highlight their respective relationships to physical material properties. We compared the model predictions to experimental observations and showed that indeed using just four linear ($S$, $n$, $G_R$ and $\lambda_R$) and three non-linear ($b$, $\delta$ and $C_1$) viscoelastic parameters are sufficient to capture the transient rheological behavior of this complex cross-linked gel to a surprising degree of accuracy over a wide range of strains $\gamma_0$ and frequencies $\omega$. We could of course relax this assumption and allow each of these modes (which represent network structures at different length scales) to exhibit different non-linear behavior. To map out these effects thoroughly, a detailed sweep of the Pipkin space shown in Figure 6 would be required to find the corresponding modal parameters ($b_k$, $\delta_k$ and $C_{1k}$).

We have also, perhaps naively, assumed an extremely simple form for describing the non-linear softening (equation (28)). One can easily imagine more sophisticated functions to describe the complex energy landscape. For example, we can increase the order of the polynomial such that:

$$\lambda_k^{-1} \sim \lambda_{k,eq}^{-1}\left(1 + C_1\left[Tr\left(\mathbf{A}_k\right) - 3\right] + C_2\left[Tr\left(\mathbf{A}_k\right) - 3\right]^2\right) \qquad (37)$$

Alternatively, other functions such as exponential, hyperbolic or even functions that include the rate of strain can be adopted. Rather than the empirical approach, Evans and Ritchie (1999) have suggested a bond dissociation model with an energy landscape that has a single energy barrier. The characteristics of this barrier are determined by both the magnitude and rate of loading of the tensile force in the elastic segments.

Finally, we note that more complex spring laws may better approximate the semi-flexible nature of the gluten chains that comprise the network segments [van den Brule (1993)]. A possible candidate is the Worm-Like Chain law (WLC) that has been used with reasonable success in describing biopolymer gel networks [Storm *et al.* (2005)]. Evans and Ritchie (1999)also investigated the force-extension behavior of a WLC when it is coupled with their non-linear network destruction equation; the resulting rate of network dissociation is of an exponential form. Currently, there exists no strong evidence to prefer one function over another and this seemingly endless list of possible modifications merely illustrates the flexibility of the transient network approach [Hyun *et al.* (2002)]. LAOS experiments over a wide range of strain amplitudes and frequencies can help in narrowing down the most appropriate functional forms.

To conclude, we note the strong similarities between this gluten gel and other bio-polymer networks in terms of the strain-stiffening observed and the ability to regain the equilibrium strength even after severe deformations and softening [Chaudhuri *et al.* (2007)]. The latter feature also bears strong resemblance to the so called reversible polymer networks that are held together by hydrogen bonding at the network junctions [Sijbesma *et al.* (1997)]. These junctions can yield before the macromolecular strands are irreversibly ruptured as a result of the application of external strain and are subsequently reformed when the material is returned to its equilibrium state. This idea can be simply demonstrated by the fact that if a gluten dough is cut into halves, the two halves can be recombined by simply holding them together. An analogous method is to disrupt the hydrogen bonds chemically with 8M urea solution; The gel can then be reconstituted by simply reintroducing water to wash out the Urea. Such similarities suggest that the multiple-mode finitely extensible network model developed here can find applications in a much a wider context.

## VII ACKNOWLEDGEMENTS

The authors wish to acknowledge Kraft Foods for financial support of this work and Prof. Eric Windhab from ETH-Zurich for encouraging us to explore the properties of gluten gels. The authors would also like to thank M. Padmanabhan for a number of stimulating conversations on the rheological properties of doughs.

## REFERENCES

Bagley, E.B., D.D. Christianson and J.A. Martindale, "Uniaxial compression of a hard wheat-flour dough - data-analysis using the upper convected Maxwell model," Journal of Texture Studies, 19(3), 289-305 (1988)

Belton, P.S., "On the elasticity of wheat gluten," Journal of Cereal Science, 29(2), 103-107 (1999)

Bird, R.B., "Teaching with FENE dumbbells," Rheology Bulletin, 76(1), 10 (2007)

Bird, R.B., R.C. Armstrong and O. Hassager, *Dynamics of Polymeric Liquids: Volume 1 Fluid Mechanics*. John Wiley & Sons, Inc, New York (1987a)

Bird, R.B., C.F. Curtiss, R.C. Armstrong and O. Hassager, *Dynamics of Polymeric Liquids: Volume 2 Kinetic Theory*. John Wiley & Sons, Inc, New York (1987b)

Bloksma, A.H., "Dough structure, dough rheology, and baking quality," Cereal Foods World, 35(2), 237-244 (1990a)

Bloksma, A.H., "Rheology of the breadmaking process," Cereal Foods World, 35(2), 228-236 (1990b)

Bowditch, N., "On the motion of a pendulum suspended from two points," Memoirs of the American Academy of Arts and Sciences, 3(2), 413-436 (1815)

Buchholz, R.H., "An epitrochoidal mixer," The Mathematical Scientist, 15, 7-14 (1990)

Chambon, F. and H.H. Winter, "Linear viscoelasticity at the gel point of a cross-linking PDMS with imbalanced stoichiometry," Journal of Rheology, 31(8), 683-697 (1987)

Charalambides, M., W. Xiao and G. Williams, "Rolling of wheat flour dough," 4th International Symposium on Food Rheology and Structure, ETH, Zurich, (2006)

Chaudhuri, O., S.H. Parekh and D.A. Fletcher, "Reversible stress softening of actin networks," Nature, 445, 295-298 (2007)

Cho, K.S., K.H. Ahn and S.J. Lee, "A geometrical interpretation of large amplitude oscillatory shear response," Journal of Rheology, 49(3), 747-758 (2005)

Considère, M., "Memoire sur l'emploi du fer et de l'acier dans les constructions," Annales des Ponts et Chausées, 9, 574–605 (1885)

Creeth, J.M., "Constituents of mucus and their separation," British Medical Bulletin, 34(1), 17-24 (1978)

Crowell, A.D., "Motion of the Earth as viewed from the Moon and the y-suspended pendulum," American Journal of Physics, 49(5), 452-454 (1981)

Dealy, J.M. and K.F. Wissbrun, *Melt rheology and its role in plastics processing : theory and applications*. Van Nostrand Reinhold, New York (1990)

Dobraszczyk, B.J., "The physics of baking: rheological and polymer molecular structure-function relationships in breadmaking," Journal of Non-Newtonian Fluid Mechanics, 124(1-3), 61-69 (2004)

Evans, E. and K. Ritchie, "Strength of a weak bond connecting flexible polymer chains," Biophysical Journal, 76(5), 2439-2447 (1999)

Ewart, J.A.D., "Hypothesis for how linear glutenin holds gas in dough," Food Chemistry, 32(2), 135-150 (1989)

Ewoldt, R.H., C. Clasen, A.E. Hosoi and G.H. McKinley, "Rheological fingerprinting of gastropod pedal mucus and synthetic complex fluids for biomimicking adhesive locomotion," Soft Matter, 3(5), 634-643 (2007)

Ewoldt, R.H., A.E. Hosoi and G.H. McKinley, "New measures for characterizing nonlinear viscoelasticity in large amplitude oscillatory shear," Journal of Rheology, 52(6), 1427-1458 (2008)

Ghosh, I., G.H. McKinley, R.A. Brown and R.C. Armstrong, "Deficiencies of FENE dumbbell models in describing the rapid stretching of dilute polymer solutions," Journal of Rheology, 45(3), 721-758 (2001)

Gittes, F. and F.C. MacKintosh, "Dynamic shear modulus of a semiflexible polymer network," Physical Review E, 58(2), R1241 (1998)

Gras, P.W., H.C. Carpenter and R.S. Anderssen, "Modelling the developmental rheology of wheat-flour dough using extension tests," Journal of Cereal Science, 31(1), 1-13 (2000)

Hibberd, G.E. and W.J. Wallace, "Dynamic viscoelastic behaviour of wheat flour doughs," Rheologica Acta, 5(3), 193-198 (1966)

Hyun, K., S.H. Kim, K.H. Ahn and S.J. Lee, "Large amplitude oscillatory shear as a way to classify the complex fluids," Journal of Non-Newtonian Fluid Mechanics, 107(1-3), 51-65 (2002)

Janmey, P.A., "A torsion pendulum for measurement of the viscoelasticity of biopolymers and its application to actin networks," Journal of Biochemical and Biophysical Methods, 22(1), 41-53 (1991)

Keunings, R., "On the Peterlin approximation for finitely extensible dumbbells," Journal of Non-Newtonian Fluid Mechanics, 68(1), 85-100 (1997)

Kokelaar, J.J., T. van Vliet and A. Prins, "Strain hardening properties and extensibility of flour and gluten doughs in relation to breadmaking performance," Journal of Cereal Science, 24(3), 199-214 (1996)

Lefebvre, J., "An outline of the non-linear viscoelastic behaviour of wheat flour dough in shear," Rheologica Acta, 45(4), 525-538 (2006)

Letang, C., M. Piau and C. Verdier, "Characterization of wheat flour-water doughs. Part I: Rheometry and microstructure," Journal of Food Engineering, 41(2), 121-132 (1999)

Lissajous, J., "Mémoire sur l'étude optique des mouvements vibratoires," Annales de Chimie et de Physique, 51, 147-231 (1857)

Ma, L.L., J.Y. Xu, P.A. Coulombe and D. Wirtz, "Keratin filament suspensions show unique micromechanical properties," Journal of Biological Chemistry, 274(27), 19145-19151 (1999)

McKinley, G.H. and O. Hassager, "The Considère condition and rapid stretching of linear and branched polymer melts," Journal of Rheology, 43(5), 1195-1212 (1999)

Ng, T.S.K. and G.H. McKinley, "Power law gels at finite strains: The nonlinear rheology of gluten gels," Journal of Rheology, 52(2), 417-449 (2008)

Ng, T.S.K., G.H. McKinley and M. Padmanabhan, "Linear to non-linear rheology of wheat flour dough," Applied Rheology, 16(5), 265-274 (2006)

Pearson, G.H. and R.W. Connelly, "The use of extensional rheometry to establish operating parameters for stretching processes," Journal of Applied Polymer Science, 27(3), 969-981 (1982)

Phan-Thien, N., M. Newberry and R.I. Tanner, "Non-linear oscillatory flow of a soft solid-like viscoelastic material," Journal of Non-Newtonian Fluid Mechanics, 92(1), 67-80 (2000)

Phan-Thien, N., M. Safari-Ardi and A. Morales-Patiño, "Oscillatory and simple shear flows of a flour-water dough: A constitutive model," Rheologica Acta, 36(1), 38-48 (1997)

Philippoff, W., "Vibrational measurements with large amplitudes," Transactions of the Society of Rheology, 10(1), 317-334 (1966)

Pipkin, A.C., *Lectures on viscoelasticity theory*. Applied mathematical sciences, v. 7. Springer, New York (1972)

Ramkumar, D.H.S., M. Bhattacharya, J.A. Menjivar and T.A. Huang, "Relaxation behavior and the application of integral constitutive equations to wheat dough," Journal of Texture Studies, 27(5), 517-544 (1996)

Rasmussen, H.K., P. Laille and K.J. Yu, "Large amplitude oscillatory elongation flow," Rheologica Acta, 47(1), 97-103 (2008)

Schofield, R.K. and G.W.S. Blair, "The relationship between viscosity, elasticity and plastic strength of a soft material as illustrated by some mechanical properties of flour dough. IV. The separate contributions of gluten and starch," Proceedings of the Royal Society of London. Series A, Mathematical and Physical Sciences, 160(900), 87-94 (1937)

Sijbesma, R.P., F.H. Beijer, L. Brunsveld, B.J.B. Folmer, J. Hirschberg, R.F.M. Lange, J.K.L. Lowe and E.W. Meijer, "Reversible polymers formed from self-complementary monomers using quadruple hydrogen bonding," Science, 278(5343), 1601-1604 (1997)

Sim, H.G., K.H. Ahn and S.J. Lee, "Large amplitude oscillatory shear behavior of complex fluids investigated by a network model: a guideline for classification," Journal of Non-Newtonian Fluid Mechanics, 112(2-3), 237-250 (2003)

Singh, H. and F. MacRitchie, "Application of polymer science to properties of gluten," Journal of Cereal Science, 33(3), 231-243 (2001)

Sliwinski, E.L., P. Kolster and T. van Vliet, "On the relationship between large-deformation properties of wheat flour dough and baking quality," Journal of Cereal Science, 39(2), 231-245 (2004)

Smith, J.R., T.L. Smith and N.W. Tschoegl, "Rheological properties of wheat flour doughs. III. Dynamic shear modulus and its dependence on amplitude, frequency, and dough composition " Rheologica Acta, 9(2), 239-252 (1970)

Storm, C., J.J. Pastore, F.C. MacKintosh, T.C. Lubensky and P.A. Janmey, "Nonlinear elasticity in biological gels," Nature, 435(7039), 191-194 (2005)

Tanner, R.I., F.Z. Qi and S.C. Dai, "Bread dough rheology and recoil I. Rheology," Journal of Non-Newtonian Fluid Mechanics, 148(1-3), 33-40 (2008)

Tee, T.T. and J.M. Dealy, "Nonlinear viscoelasticity of polymer melts," Transactions of the Society of Rheology, 19(4), 595-615 (1975)

Treloar, L.R.G., *The physics of rubber elasticity*. Oxford University Press, Oxford (2005)

Uthayakumaran, S., M. Newberry, M. Keentok, F.L. Stoddard and F. Bekes, "Basic rheology of bread dough with modified protein content and glutenin-to-gliadin ratios," Cereal Chemistry, 77(6), 744-749 (2000)

Uthayakumaran, S., M. Newberry, N. Phan-Thien and R. Tanner, "Small and large strain rheology of wheat gluten," Rheologica Acta, 41(1-2), 162-172 (2002)

van den Brule, B., "Brownian dynamics simulation of finitely extensible bead spring chains," Journal of Non-Newtonian Fluid Mechanics, 47, 357-378 (1993)

van Vliet, T., A.M. Janssen, A.H. Bloksma and P. Walstra, "Strain-hardening of dough as a requirement for gas retention," Journal of Texture Studies, 23(4), 439-460 (1992)

Wang, C.F. and J.L. Kokini, "Simulation of the nonlinear rheological properties of gluten dough using the Wagner constitutive model," Journal of Rheology, 39(6), 1465-1482 (1995)

Wilhelm, M., "Fourier-Transform rheology," Macromolecular Materials and Engineering, 287(2), 83-105 (2002)

Winter, H.H. and F. Chambon, "Analysis of linear viscoelasticity of a cross-linking polymer at the gel point," Journal of Rheology, 30(2), 367-382 (1986)

Winter, H.H. and M. Mours, *Rheology of polymers near liquid-solid transitions*, in *Neutron Spin Echo Spectroscopy, Viscoelasticity, Rheology (Advances in Polymer Science vol. 134)*. 1997, Springer Berlin / Heidelberg. p. 165-234.

Wyss, H.M., K. Miyazaki, J. Mattsson, Z.B. Hu, D.R. Reichman and D.A. Weitz, "Strain-rate frequency superposition: A rheological probe of structural relaxation in soft materials," Physical Review Letters, 98(23), 238303 (2007)

Zou, Q., S.M. Habermann-Rottinghaus and K.P. Murphy, "Urea effects on protein stability: Hydrogen bonding and the hydrophobic effect," Proteins-Structure Function and Genetics, 31(2), 107-115 (1998)